

RESEARCH ARTICLE



Decoding the RNA virome of the tree parasite *Armillaria* provides new insights into the viral community of soil-borne fungi

Wajeeha Shamsi¹ | Renate Heinzelmann¹ | Sven Ulrich¹ |
Hideki Kondo² | Carolina Cornejo¹

¹Swiss Federal Institute for Forest, Snow, and Landscape Research WSL, Birmensdorf, Switzerland

²Institute of Plant Science and Resources, Okayama University, Kurashiki, Japan

Correspondence

Wajeeha Shamsi and Carolina Cornejo, Swiss Federal Institute for Forest, Snow and Landscape Research WSL, Zuercherstrasse 111, 8903 Birmensdorf, Switzerland.
Email: wajeeha.shamsi@wsl.ch and carolina.cornejo@wsl.ch

Funding information

Swiss Federal Institute for Forest, Snow and Landscape Research; WSL Internal Grant, Grant/Award Number: 202111N2343

Abstract

The globally distributed basidiomycete genus *Armillaria* includes wood decomposers that can act as opportunistic parasites, causing deadly root rot on woody plants. To test whether RNA viruses are involved in this opportunistic behaviour, a large isolate collection of five *Armillaria* species collected over 40 years in Switzerland from trees, dead wood and soil was analysed. De novo assembly of RNA-Seq data revealed 21 viruses, 14 of which belong to putative new species. Two dsRNA viruses and an unclassified *Tymovirales* are formally described for the first time for *Armillaria*. One mitovirus occurred with a high prevalence of 71.1%, while all other viruses were much less prevalent (0.6%–16.9%). About half of all viruses were found only in one fungal species, others occurred in 2–6 fungal species. Co-infections of 2–7 viruses per isolate were not uncommon (34.9%), and most viruses persisted circulating within fungal populations for decades. Some viruses were related to viruses associated with other *Armillaria* species, supporting the hypothesis that virus transmission can occur between different fungal species. Although no specific correlation between viruses and the fungal trophic strategy was found, this study opens new insights into viral diversity hidden in the soil microbiome.

INTRODUCTION

Soil ecosystems are the major reservoir of species diversity on earth, and fungi are the group with the highest proportion of soil inhabitants, with 90% of all known fungal species living in soil (Anthony et al., 2023). All soil-borne microbial groups, including bacteria, archaea, protozoa, algae, fungi and oomycetes, harbour viruses—intracellular infectious agents depending on a living host cell for replication (Sutela et al., 2019). However, in comparison to plant viruses (discovered in 1892), animal viruses (1898) and bacteriophages (1915/1917), fungal viruses (mycoviruses) were discovered relatively late and therefore are still poorly understood. Since their first

description in 1962 in the basidiomycete fungus *Agaricus bisporus* many new groups of mycoviruses have been identified in filamentous fungi and fungal-like organisms thanks to advancements in sequencing technology (Botella et al., 2020; Hollings & Stone, 1971; Koonin et al., 2023; Sato et al., 2020; Vainio et al., 2017). Resident mainly in the cytoplasm or mitochondria, rarely in the nucleus, mycoviruses are usually cryptic, with latent infection and no visible effect on the host fungus (Ghabrial et al., 2015), but a growing number of mycoviruses show complex relationships with their host (Kondo et al., 2022; Wolf et al., 2018). Some mycoviruses confer beneficial effects on the host (Ahn & Lee, 2001; Fuke et al., 2011; Thapa et al., 2016), while

This is an open access article under the terms of the [Creative Commons Attribution-NonCommercial-NoDerivs](https://creativecommons.org/licenses/by-nc-nd/4.0/) License, which permits use and distribution in any medium, provided the original work is properly cited, the use is non-commercial and no modifications or adaptations are made.

© 2024 The Authors. *Environmental Microbiology* published by Applied Microbiology International and John Wiley & Sons Ltd.

others have the potential to reduce the virulence of phytopathogenic fungi such as *Cryphonectria parasitica*, *Sclerotinia sclerotiorum* and *Rosellinia necatrix* (Xie & Jiang, 2014). Such hypovirulent mycoviruses are of particular interest as biological control agents (Prospero et al., 2021), and recently several soil-borne fungal pathogens were screened for mycoviruses including *Heterobasidion* spp. infecting conifers (Vainio, 2019; Vainio & Hantula, 2016), the fruit tree pathogen *R. necatrix* (Arjona-Lopez et al., 2018; Kondo et al., 2013; Telengech et al., 2020) as well as fungi from the genus *Armillaria* (Linnakoski et al., 2021).

Armillaria species and species from the sister genus *Desarmillaria* (Physalacriaceae, Agaricales) are soil-borne basidiomycetes with a worldwide distribution. The parasitic *Armillaria* and *Desarmillaria* species are dreaded necrotrophic tree root pathogens that can colonize the host root tissue of woody plants and cause root system decay. However, all *Armillaria* species can also feed on dead wood and thus play an important ecological role as decomposers in woody ecosystems (Baumgartner et al., 2011; Heinzelmänn et al., 2019). Of the more than 40 described species (Kim et al., 2022), five *Armillaria* and two *Desarmillaria* fungi occur in Europe (Guillaumin et al., 1993; Marxmüller & Guillaumin, 2005). They include *Armillaria mellea* and *Armillaria ostoyae*, which are important primary pathogens (infecting healthy hosts) and cause significant mortality and economic losses not only in forests, fruit tree plantations, orchards and vineyards but also in urban green spaces such as parks and gardens throughout the Northern Hemisphere (Cromey et al., 2020; Guillaumin et al., 1989; Guillaumin et al., 1993; Kile et al., 1991). Similarly, *Desarmillaria tabescens* can also act locally as an aggressive primary pathogen (Guillaumin et al., 1993). Although the other *Armillaria* species in Europe mostly act as secondary pathogens (infecting trees weakened by other biotic or abiotic stressors) or feed saprotrophically, *Armillaria cepistipes* and *Armillaria gallica* have recently attracted attention for accelerating the decline of ash trees in Europe due to their interaction with the invasive ascomycete *Hymenoscyphus fraxineus*, the causal agent of the ash dieback disease (Enderle et al., 2017; Gross et al., 2014; Madsen et al., 2021; Marçais et al., 2016). Another interesting feature of *Armillaria* species is the ability to form rhizomorphs, root-like fungal structures that in some species form large and dense networks in forest soils (Prospero, Holdenrieder, & Rigling, 2003; Tsykun et al., 2012). *Armillaria* species can colonize a large area of several hectares, in extreme cases multiple square kilometres, and may last for multiple forest generations (Bendel, Kienast, & Rigling, 2006; Ferguson et al., 2003; Smith et al., 1992).

Controlling *Armillaria* root disease is challenging because the fungus lives hidden in the soil and root system of infected trees and can also endure a long time in woody debris (Coetzee et al., 2001; Kedves

et al., 2021; Redfern & Filip, 1991; Travadon et al., 2012). Therefore, Linnakoski et al. (2021) recently argued that the large clonal individuals living in the soil may be optimal targets for the application of viral biocontrol agents and, thus, confirmed by RNA-Sequencing of *Armillaria* species the presence of four single-stranded (ss) RNA viruses in the secondary pathogens *Armillaria borealis* and *A. cepistipes* from Finland, while the other nine detected ssRNA viruses were from other regions of the world (Siberia, South Africa, The United States, Asia, Australia and Oceania). Remarkably, eight of the 13 RNA viruses detected were ambi-like viruses, which have recently been reported as unique circular ssRNA viruses (Forgia et al., 2023). These results clearly indicated that *Armillaria* isolates from unexplored geographic regions may conceal unforeseen viral diversity that has not yet been discovered.

In the present study, we aimed to expand our understanding of the species diversity of *Armillaria*-associated viruses in time and space. To achieve this goal, we examined the presence of RNA viruses in a large number of isolates from five European *Armillaria* and one *Desarmillaria* species collected over the past 40 years from infected trees, dead wood and soil from a wide range of natural and urban habitats in Switzerland and some neighbouring countries. In previous studies, the virulence of isolates in our WSL fungal collection was experimentally assessed and gradually classified from avirulent to virulent phenotypes (Heinzelmänn et al., 2017; Prospero et al., 2004). Therefore, an important objective of this study was to assess whether mycoviruses might be involved in the virulence gradient among tested fungal isolates observed in our collection. Thus, we were particularly interested in comparing the virome of species that function as primary pathogens as opposed to species that function mainly as secondary pathogens. The virome data described in this study provide an overview of the viral community present in *Armillaria* in Central Europe over 40 years, including new RNA viruses of described or recently proposed families and an unclassified positive-sense (+) ssRNA virus.

EXPERIMENTAL PROCEDURES

Fungal isolates and virulence

A total of 166 isolates from five *Armillaria* species ($N = 164$): *A. borealis* ($N = 22$), *A. cepistipes* ($N = 17$), *A. gallica* ($N = 20$), *A. mellea* ($N = 38$) and *A. ostoyae* ($N = 67$) and *D. tabescens* ($N = 2$) were used for the present study (Table S1). The samples were collected between 1983 and 2021 in Switzerland ($N = 150$), France ($N = 6$), Italy ($N = 2$), Spain ($N = 2$), Germany ($N = 1$), the Principality of Liechtenstein ($N = 1$) and

the country of origin for four isolates collected in the 1990s was not documented (Table S1). Most isolates examined (107/166) were from primary pathogens (*A. ostoyae*, *A. mellea* and *D. tabenscens*), while the remainder (59/166) were from secondary pathogens or saprotrophs (*A. borealis*, *A. cepistipes* and *A. gallica*) (Table S1). In previous studies, the virulence of a subset of isolates was assessed experimentally by inoculation of potted seedlings: 10/22 strains of *A. borealis*, 17/17 *A. cepistipes* and 15/66 *A. ostoyae* (Heinzelmann et al., 2017; Prospero et al., 2004). Finally, for the present study, the same method of inoculation of potted seedlings was applied to 16/36 strains of *A. mellea* (Table S2).

Total RNA extraction

All isolates were stored in the WSL culture collection, revived on diamalt agar (20 g/L Diamalt, Hefe Schweiz, Stettfurt, Switzerland; 15 g/L plant propagation agar, Condalab, Madrid, Spain) and incubated for 1 week at room temperature in the dark. About 10–12 squares of 5 × 5 mm per plate were cut out and incubated in a 500 mL Erlenmeyer flask containing liquid Diamalt yeast medium (20 g/L Diamalt; 15 g/L Yeast Extract, Sigma-Aldrich, Buchs, Switzerland) in the dark and at room temperature for 7 days on a shaker. The cultures were subsequently harvested by filtration, lyophilized and the mycelium was ground manually with mortar and pestle using liquid nitrogen. The total RNA of 60 mg ground mycelium was obtained using the Spectrum™ Plant Total RNA-Kit (Sigma-Aldrich) according to the manufacturer's instructions. The RNA samples were pooled (15 samples in pools 1–3, 14 samples in pool 4, 12 samples in pools 5–12 and 11 samples in pool 13; 3.2–4.0 µg RNA/pool) and sent to Macrogen Inc. (Macrogen Europe) for library preparation (Illumina TruSeq Stranded Total RNA library construction with Ribo-Zero treatment) and sequencing on the Illumina platform NovaSeq (100 nt paired-end sequencing run; 100 M reads/sample). A total of 98.5–105.7 million reads (101 nt paired-end reads) were obtained per pool. After RNA-sequencing (RNA-seq), the reads were mapped to the reference genome of *A. gallica* (GenBank assembly accessions: GCA_012064365 and MH878687 for the latest versions of *A. gallica* genomic and partial mitochondrion genome sequences) using CLC Genomics Workbench v22 (CLC Bio-QIAGEN, Aarhus, Denmark) to identify reads of fungal origin, which were excluded from further analyses.

Detection and sequencing of viral RNA

The non-fungal sequencing reads were assembled de novo (contig number per pool: 22,678–42,747) using

CLC Genomics Workbench version 22 (CLC Bio-Qiagen, Aarhus, Denmark) using default parameters (minimum contig length = 200; mismatch cost = 2; length fraction = 0.5; similarity fraction = 0.8). Next, the Basic Local Alignment Search Tool (BLAST) was used with viral reference sequences from the National Centre for Biotechnology Information (NCBI, <https://ncbi.nlm.nih.gov/>, accessed on 22 May 2022) to screen for viral sequence contigs. Ambivirus-like sequences from public datasets were also used as queries for BLAST searches against assembled contigs generated in this study to detect further virus-related sequences.

To confirm the viral RNA detected by RNA-seq, sequence-specific primers in a range of 500–600 bp amplicon size were designed using CLC Main Workbench v22 (CLC Bio-QIAGEN) based on the sequence contigs and tested in silico using the Primer-BLAST option 'fungi (taxid:4751)' in the NCBI suite to exclude non-specific binding to fungal DNA (Table S3). After confirming the specificity of the primers in silico, the presence of viral RNA was checked in all 166 fungal strains by one-step Reverse Transcription (RT)-PCR using the PrimeScript OneStep RT-PCR v2 kit (Takara Bio Europe SAS, Saint-Germain-en-Laye, France) as described previously (Urayama et al., 2014). All reactions were subjected to the same protocol, which included DNase treatment (dsDNase, Thermo Fisher Scientific) of single RNA extracts, followed by a cDNA synthesis step at 50°C and a PCR reaction: 33 cycles of 30 s 94°C/30 s 55°C/2 min 72°C. To verify the natural character of RNA-seq contigs that were found in different fungal isolates but in the same RNA-seq library, we partially sequenced the RdRP coding region from representative isolates of selected viruses using the same primer designed for RT-PCR tests (Table S3). Total RNA extracts of selected virus-positive fungal strains were subjected to cDNA synthesis (Maxima First Strand cDNA Synthesis Kit, Thermo Fisher Scientific) and a PCR reaction using the GoTaq Flexi DNA Polymerase (Promega Corporation), which included an initial denaturation of 2 min at 95°C, followed by 35 cycles of 30 s 95°C/30 s 55°C/2 min 72°C and a final extension of 10 min at 72°C. PCR amplicons were verified by Sanger sequencing using the BigDye Terminator v3.1 Cycle Sequencing Kit (Thermo Fisher Scientific) and the resulting forward and reverse strands were assembled using the software CLC Main Workbench. To obtain the nucleotide sequences at the 5' and 3' termini and complete the viral contigs, RNA-ligase-mediated rapid amplification of cDNA ends (RLM-RACE) was used as described previously (Jamal et al., 2019). The RACE-PCR products were ligated into pGEMT-Easy (Promega, Madison, WI) and transformed into *Escherichia coli* DH5α competent cells (Takara Bio Inc., Shiga, Japan) for Sanger sequencing. The primer sequences used in RLM-RACE were designed at the 5' and 3' flanking regions using the

CLC Main Workbench listed in Table S3. The viral sequences reported in this study were deposited in the Genbank/ENA/DDBJ database with accession numbers OQ749606–OQ749611 and OR670528–OR670538 (Bioproject PRJNA1017781).

Characterization of mycoviruses

To detect potential open reading frames (ORFs) in the viral contigs and identify conserved domains in the ORFs, the ORF finder program, which applies the standard or yeast mitochondrial genetic code, and the conserved domain database (CDD) (Marchler-Bauer et al., 2016) of the NCBI suite were used. Sequence similarity searches were performed using both BLASTx and BLASTp programs in NCBI. The percent identity matrix was created using the online CLUSTAL Omega tool (<https://www.ebi.ac.uk/Tools/msa/clustalo/>).

The maximum likelihood (ML) method was employed to perform phylogenetic analysis of the deduced virus polypeptides (RNA-dependent RNA polymerase, RdRP). The online MAFFT server v7 (<https://mafft.cbrc.jp/alignment/server/>) (Katoh & Toh, 2008) was used to align the virus sequences and subsequently, PhyML 3.0 to generate ML trees with automatic smart model selection (SMS Model Selection) (Guindon et al., 2010). Branch supports were calculated based on 1000 bootstrap repetitions and the tree was visualized using Fig-Tree v1.4.4 (<http://tree.bio.ed.ac.uk/software/>).

Secondary structures at the 5' and 3' terminal regions were predicted by RNA structure software v6.4 (Mathews et al., 2004) (<https://rna.urmc.rochester.edu/RNAstructure.html>).

RESULTS

Diversity and prevalence of RNA viruses in *Armillaria* species

Local BLAST analysis revealed 91 de novo assembled virus-like contigs ranging in length from 251 to 11,451 nucleotides (nt) in the 13 pooled samples. Among them, we detected at least 21 candidate RNA viruses with complete or nearly-complete genomes (Table 1), including mitoviruses (family *Mitoviridae*), ourmia-like viruses (*Botourmiaviridae*), negative-sense (–) ssRNA mymonaviruses (*Mymonaviridae*), a double-stranded (ds) RNA partitivirus (*Partitiviridae*) and also unclassified RNA viruses: including a dsRNA virus (proposed family ‘Phlegiviridae’) (Sato et al., 2023), a (+) ssRNA virus (unclassified *Tymovirales*), and viruses related to ambi- or ambi-like viruses that are circular ssRNA viruses of the four proposed families (‘Dumbiviridae’, ‘Quambiviridae’, ‘Trimbiviridae’ and ‘Unambiviridae’) in the phylum Ambiviricota of the order ‘Crytulvirales’ (Turina et al., 2023). Some

additional incomplete virus-like fragments were not considered further in this study.

Two mitoviruses, seven ambi-like viruses and one phlegivirus occurred in multiple fungal species, whereas the others were each detected only in one fungal species (Table 2). Due to the high similarity of amino acid sequences (aa), 7 of the viruses listed in Table 1 were considered to be variants of already known mycoviruses (Linnakoski et al., 2021), and 14 are newly described below.

Genome characterization of *Armillaria*-associated viruses

Mitoviruses

The RNA-seq data revealed 17 putative virus-like contigs with potential complete coding sequences that shared similarities to previously reported mitovirids. Of these, nine de novo assembled contigs shared 87.5%–96.7% identity at the nucleotide (nt) level and were thus considered variants of the same mitovirid (Figure S1a). RT-PCR results indicated that 118 fungal isolates (71.1%) were positive for this mitovirus and that it occurred in all tested *Armillaria* species. The virus had a high prevalence in all tested species (64.2%–100%), except for *A. borealis* (18.2%) (Table 2). Based on its high aa identity, the virus was considered a variant of the *Armillaria borealis* mitovirus 1 (AbMV1, 2011A isolate) sequence found in the GenBank record (accession number ON875998) (Table 1 and see also below).

The remaining eight contigs shared 87.4%–96.7% identity at the nucleotide level and were considered variants of another mitovirid (Figure S1b). In total, eight isolates of *A. borealis*, *A. cepistipes*, *A. gallica* and *A. ostoyae* were positive for this mitovirid (Table 2). This virus was tentatively named *Armillaria* mitovirus 1 (AMV1, accession number OQ749609).

The (+)ssRNA genome of AbMV1 was 3171 nt in length (complete genome) that encoded one large 720 aa (molecular mass 82.0 kDa) long ORF. AMV1 encoded two ORFs, a smaller ORF (s-ORF) of 139 aa and a second large ORF of 1150 amino acids (aa) (129.1 kDa) when the mitochondrial codon usage was applied. The conserved domain for RdRP (Mitovir_RNA_pol superfamily; cl05469) was located at positions 1482–2222 nt (AbMV1) and 1592–2962 nt (AMV1), respectively (Figure 1A). No hits were found in the BLASTx analysis of s-ORF of AMV1. A stem-loop structure was predicted in the long 5' untranslated region (UTR) of AbMV1 and AMV1 genomic RNA (Figure S1c).

Characteristic conserved motifs of mitoviruses were also detected in the RdRP-based alignment of AbMV1 and AMV1 with other selected mitoviruses (Figure S1d). In the BLASTp search, AbMV1 exhibited 83.2% identity with the AbMV1 2011A isolate and AMV1 exhibited

TABLE 1 Mycoviruses detected in *Armillaria* isolates from Switzerland and neighbouring countries, based on best match by BLASTp search.

Virus name (size)	Contig no.	Total read count ^a	Genome type/segment	aa identity (%)	Cover (%)	Top BLASTp hit RdRP (accession number)	Host fungus strain
<i>Armillaria borealis</i> mitovirus 1 (AbMV1) ^b (3171 nt) ^c	Arm_P5-c38	794,142	(+)ssRNA	83.2	100	<i>Armillaria borealis</i> mitovirus 1 (WEA82906)	<i>Armillaria</i> sp.
<i>Armillaria</i> mitovirus 1 (AMV1) (4378 nt)	Arm_P1-c69	456,096	(+)ssRNA	68.8	96	<i>Armillaria mellea</i> mitovirus 1 (WNH24567)	<i>Armillaria mellea</i> Geyve
<i>Armillaria mellea</i> ourmia-like virus 1 (AmOIV1) ^d (3919 nt)	Arm_P3-c63	20,684	(+)ssRNA	96.9	90	<i>Armillaria mellea</i> ourmia-like virus 1 (YP_010805005)	<i>Armillaria mellea</i> CMW50256
<i>Armillaria mellea</i> ourmia-like virus 2 (AmOIV2) ^d (3162 nt)	Arm_P7-c718	15,993	(+)ssRNA	96.4	100	<i>Armillaria mellea</i> ourmia-like virus 2 (YP_010805006)	<i>Armillaria mellea</i> CMW3973
<i>Armillaria ostoyae</i> ourmia-like virus 1 (AoOIV1) (2984 nt)	Arm_P11-c1722	9932	(+)ssRNA	65.7	97	<i>Armillaria mellea</i> ourmia-like virus 2 (YP_010805006)	<i>Armillaria mellea</i> CMW3973
<i>Armillaria ostoyae</i> RNA virus 1 (AoRV1) (8708 nt)	Arm_P8-c66	59,182	(+)ssRNA	42.1	76	Bramycfau virus 2 (UQS94368)	<i>Mycetophylax faunulus</i> WM17012805 Antswm17012805
<i>Armillaria gallica</i> negative-stranded RNA virus 1 (AgNSRV1) (11,466 nt) ^c	Arm_P2-c408	6425	(-)ssRNA	53.2	99	<i>Armillaria mellea</i> negative-stranded RNA virus 2 (DAD54832)	<i>Armillaria mellea</i> ELDO17
<i>Armillaria cepistipes</i> negative-stranded RNA virus 1 (AcNSRV1) (11,016 nt)	Arm_P3-c525	20,339	(-)ssRNA	53.2	97	<i>Armillaria mellea</i> negative-stranded RNA virus 1 (YP_010805004)	<i>Armillaria mellea</i> CMW3973
<i>Armillaria mellea</i> negative-stranded RNA virus 1 (AmNSRV) ^d (10,646 nt)	Arm_P7-c318	657	(-)ssRNA	97.0	100	<i>Armillaria mellea</i> negative-stranded RNA virus 1 (YP_010805004)	<i>Armillaria mellea</i> CMW3973
<i>Armillaria gallica</i> partitivirus 1 (AgPV1) (1755 bp) ^c	Arm_P2-c5351	428	dsRNA1	65.6	99	<i>Flammulina velutipes</i> isometric virus (BAH08700)	<i>Flammulina velutipes</i> isolate No. 6
(1767 bp) ^c	Arm_P2-c2331	862	dsRNA2	21.6	78	<i>Grosmannia clavigera</i> partitivirus 1 (AZT88607)	<i>Grosmannia clavigera</i> strain KW1407
<i>Armillaria</i> RNA virus 1	Arm_P13-c264	50,226	dsRNA	35.5	29	<i>Sclerotium rofsii</i> mycovirus dsRNA1 (AZF86106)	<i>Sclerotium rofsii</i> strain BLH-1

(Continues)

TABLE 1 (Continued)

Virus name (size)	Contig no.	Total read count ^a	Genome type/segment	aa identity (%)	Cover (%)	Top BLASTp hit RdRP (accession number)	Host fungus strain
(ARV1) (11,806 bp) ^c							
Armillaria spp. ambi-like virus 5 (AsAIV5) (4772 nt) ^e	Arm_P4-c182	27,815	ssRNA ^f	65.6	99	Armillaria mellea ambi-like virus 1 (DAD54837)	Armillaria mellea strain ELDO17
Armillaria spp. ambi-like virus 6 (AsAIV6) (4511 nt)	Arm_P6-c310	89,033	ssRNA ^f	76.3	99	Armillaria mellea ambi-like virus 2 (DAD54839)	Armillaria mellea (no information on strain)
Armillaria spp. ambi-like virus 7 (AsAIV7) (4533 nt)	Arm_P1-c53	108,520	ssRNA ^f	83.9	99	Armillaria borealis ambi-like virus 2 (QUD20368)	Armillaria borealis strain Ab4B
Armillaria spp. ambi-like virus 8 (AsAIV8) (4838 nt)	Arm_P4-c178	5474	ssRNA ^f	62.3	94	Armillaria novae-zelandiae ambi-like virus 1 (DAD54841)	Armillaria novae-zelandiae strain 2840
Armillaria ambi-like virus 3 (AAIV3) ^d (4385 nt)	Arm_P4-c50	13,853	ssRNA	99.0	100	Armillaria ambi-like virus 3 (QUD20379)	Armillaria borealis strain Ab9A
Armillaria spp. ambi-like virus 3 (AsAIV3) ^b (4506 nt)	Arm_P3-c40	77,473	ssRNA	99.4	100	Armillaria spp. ambi-like virus 3 (WCL23002)	Armillaria spp. (no information on strain)
Armillaria borealis ambi-like virus 2 (AbAIV2) ^d (4528 nt)	Arm_P1-347	5361	ssRNA	98.4	100	Armillaria borealis ambi-like virus 2 (QUD20368)	Armillaria borealis strain Ab4B
Armillaria mellea ambi-like virus 3 (AmAIV3) (4814 nt) ^c	Arm_P5-c89	108,859	ssRNA	81.1	97	Armillaria borealis ambi-like virus 1 (QUD20357)	Armillaria borealis strain N40
Armillaria mellea ambi-like virus 4 (AmAIV4) (4417 nt) ^e	Arm_P5-c177	69,712	ssRNA	86.6	100	Armillaria spp. ambi-like virus 3 (WCL23002)	Armillaria spp. (no information on strain)
Armillaria mellea ambi-like virus 5 (AmAIV5) (4525 nt)	Arm_P5-c88	70,631	ssRNA	75.7	99	Armillaria mellea ambi-like virus 2 (DAD54839)	Armillaria mellea (no information on strain)

^aThe number of raw reads mapping to the virus sequences were obtained by the Read Mapping algorithm via CLC Genomic Workbench with the following parameters: length fraction = 0.9; and similarity fraction = 0.95.

^bSequence record only given in GenBank, but not reported in a publication.

^cComplete genome sequence.

^dVariants of the viruses reported by Linnakoski et al. (2021).

^eWith undetermined nucleotide sequences (NNN).

^fReported ambiviruses have a circular ssRNA genome with self-cleaving elements (Forgia et al., 2023).

TABLE 2 Frequency of individual RNA viruses detected in *Armillaria* isolates in this study.

Viruses	<i>Armillaria</i> spp.						Overall (N = 166)
	<i>A. borealis</i> (N = 22)	<i>A. gallica</i> (N = 20)	<i>A. cepistipes</i> (N = 17)	<i>A. mellea</i> (N = 38)	<i>A. ostoyae</i> (N = 67)	<i>D. tabescens</i> (N = 2)	
AbMV1 ^a	4 (18.2%) ^b	18 (90%)	17 (100.0%)	34 (89.5%)	43 (64.2%)	2 (100.0%)	118 (71.1%)
AMV1	1 (4.5%)	3 (15.0%)	2 (11.8%)	0	2 (3.0%)	0	8 (4.8%)
AmOIV1 ^a	0	0	6 (35.3%)	0	0	0	6 (3.6%)
AmOIV2 ^a	0	0	0	1 (2.6%)	0	0	1 (0.6%)
AoOIV1	0	0	0	0	1 (1.5%)	0	1 (0.6%)
AoRV1	0	0	0	0	3 (4.5%)	0	3 (1.8%)
AgNSRV1	0	1 (5.0%)	0	0	0	0	1 (0.6%)
AcNSRV1	0	0	1 (5.9%)	0	0	0	1 (0.6%)
AmNSRV1 ^a	0	0	0	8 (21.1%)	0	0	8 (13.3%)
AgPV1	0	1 (5.0%)	0	0	0	0	1 (0.6%)
ARV1	1 (4.5%)	2 (10.0%)	0	0	2 (3.0%)	0	5 (3.0%)
AsAIV5	0	5 (25.0%)	1 (5.9%)	6 (15.8%)	0	0	12 (7.2%)
AsAIV6	1 (4.5%)	0	0	8 (21.1%)	0	0	9 (5.4%)
AsAIV7	6 (27.3%)	0	0	20 (52.6%)	2 (3.0%)	0	28 (16.9%)
AsAIV8	1 (4.5%)	1 (5.0%)	0	0	0	0	2 (1.2%)
AAIV3 ^a	4 (18.2%)	2 (10.0%)	9 (52.9%)	0	3 (4.5%)	0	18 (10.8%)
AsAIV3 ^a	0	3 (15.0%)	6 (35.3%)	1 (2.6%)	1 (1.5%)	0	11 (6.6%)
AbAIV2 ^a	3 (13.6%)	0	1 (5.9%)	0	0	0	4 (2.4%)
AmAIV3	0	0	0	20 (52.6%)	0	0	20 (12.0%)
AmAIV4	0	0	0	13 (34.2%)	0	0	13 (7.8%)
AmAIV5	0	0	0	7 (18.4%)	0	0	7 (4.2%)

^aVariants of viruses previously reported by Linnakoski et al. (2021) or deposited in GenBank.

^bNumber of virus-positive isolates and their frequency (in parentheses) within fungal species or overall species.

68.8% identity with *Armillaria mellea* mitovirus 1 (Table 1). Based on the International Committee on Taxonomy of Viruses (ICTV) species demarcation criterion for mitoviruses (<70% RdRP aa identity) (Botella et al., 2021) and phylogenetic analysis of the deduced polypeptide (Figure 1B), AbMV1 was regarded as a variant of the unpublished mitovirus but previously deposited in GenBank, and AMV1 could be considered a new virus in the established genera *Unuamitovirus* and *Duamitovirus*, respectively, of the family *Mitoviridae*.

Ourmia-like virus

Along with the sequences of two known ourmia-like viruses (*Armillaria mellea* ourmia-like virus 1, AmOIV1 and *Armillaria mellea* ourmia-like virus, AmOIV2) in genus *Magoulivirus*, an additional ourmiavirus-like contig was detected (Table 1). A single French isolate of *A. ostoyae* (M10666) was confirmed to be positive for this virus candidate by RT-PCR (Table S1). The virus was tentatively named *Armillaria ostoyae* ourmia-like virus 1 (AoOIV1, accession number OR670528).

The AoOIV1 contig was 2984 nt long and a complete coding sequence encoded a 713 aa long ORF

(molecular mass 81.1 kDa) (Figure 2A) with an RdRP domain (ps-ssRNAv-RdRp-like superfamily; cl40470) at nt position 965–1606 (Figure 2A) that had 65.7% aa identity with the RdRP of AmOIV2 in a BLASTp search (Table 1). AoOIV1 shared eight conserved motifs with reported botourmiaviruses in the RdRP-based alignment (Figure S2). Phylogenetically, the virus clustered with members of the genus *Magoulivirus* in the family *Botourmiaviridae* (Figure 2B). Based on our analysis and the ICTV species demarcation criterion for botourmiaviruses (<90% RdRP identity) (Ayllón et al., 2020), we propose AoOIV1 as a novel member of the genus *Magoulivirus* in the family *Botourmiaviridae*.

Unclassified (+)ssRNA virus

In BLASTp search, the virus-like contig Arm_P8-c66 showed low levels of sequence identity (~42.1% aa RdRP identity) to (+)ssRNA virus-like sequences of meta-genome assemblies associated with two fungus-farming ants (*Mycetophylax faunulus* and *Paratrachymyrmex diversus*) (Table 1). Three isolates of *A. ostoyae* (Swiss isolates M5356 and M5358, and French isolate M10666) were positive for this virus candidate in RT-PCR analysis (Table S1).

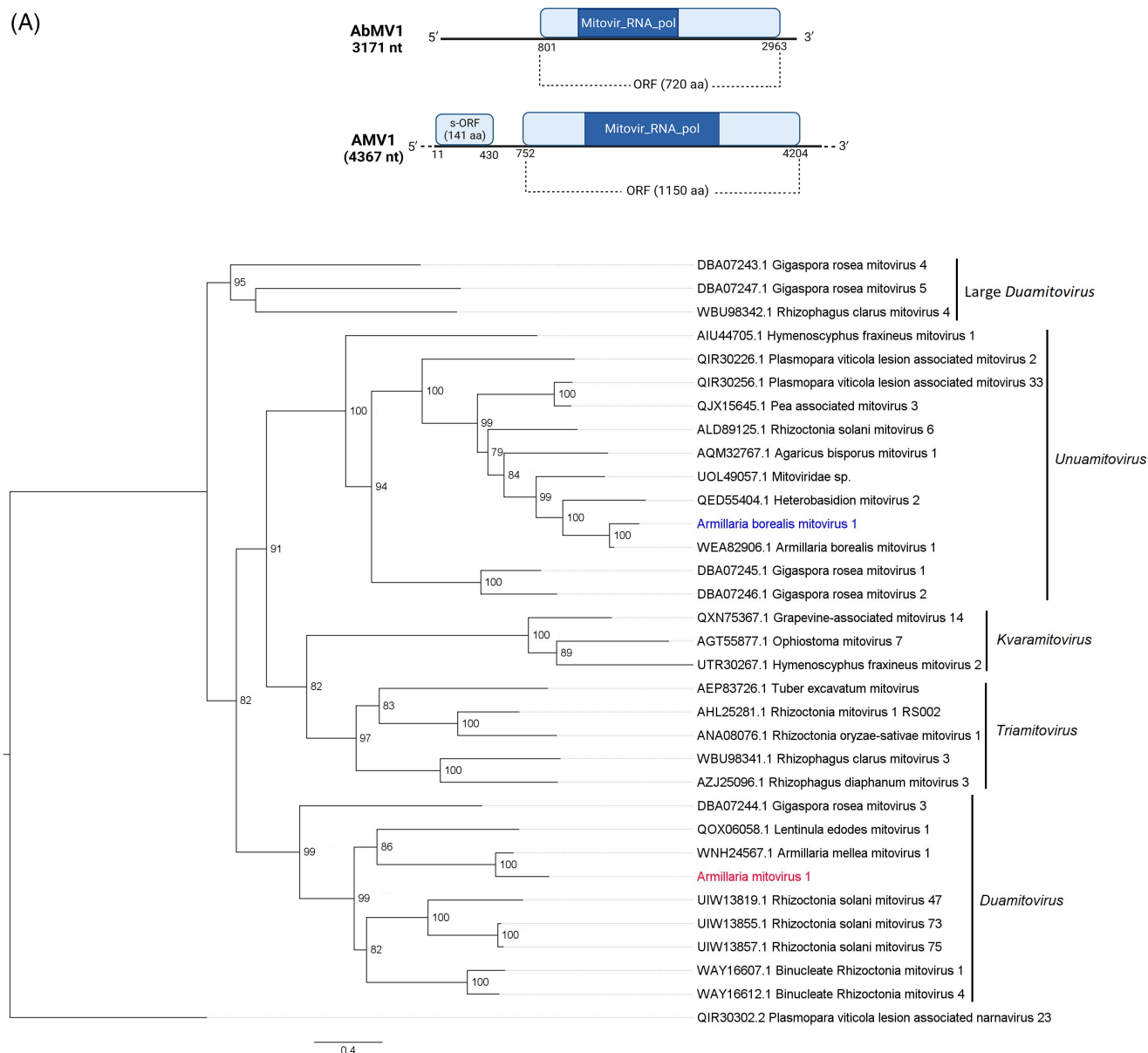


FIGURE 1 Genome organization and phylogeny of two mitoviruses from *Armillaria* isolates. (A) Schematic representation of the AbMV1 and AMV1 (+)ssRNA genomes. The ORF is represented in blue and the RdRP domain is shown in darker shade. (B) The maximum-likelihood phylogenetic tree of AbMV1 and AMV1 with selected members of four genera (*Duamitovirus*, *Kvaramitovirus*, *Triamitovirus* and *Unuamitovirus*) and large duamitoviruses (Ezawa et al., 2023) in the family *Mitoviridae*. The tree was generated from the amino acid sequence alignment of the deduced RdRPs. The novel virus is shown in red and a published virus variant is shown in blue. A narna-like virus (Plasmopara viticola lesion associated with narnavirus 23) is used as an outgroup to root the tree. Numbers at nodes are bootstrap values out of 1000 replicates. Bootstrap values (%) <60 are not shown.

The (+)ssRNA virus-like contig was 8685 nt in length, excluding the poly (A) tail, and the complete coding sequence encoded a long ORF of 2526 aa (molecular mass 291.0 kDa) and two small ORFs of 168 and 82 aa (18.6 and 9.5 kDa) in length, respectively (Figure 3A). Three conserved domains were found in the large ORF: a methyltransferase domain (Vmethyltransf superfamily; cl03298) at aa position 636–921, an RNA helicase domain (Viral_helicase 1 superfamily; cl26263) at aa position 1592–1861 and an RdRP domain (cl40470) at aa position 2182–2359

(Figure 3A). No significant similarity was found in the small ORFs in BLASTp searches. The phylogenetic analysis grouped the virus in a clade together with ant-associated viruses (Brupardiv and Bramycfau viruses) and unclassified mycoviruses (e.g., *Agaricus bisporus* viruses; Deakin et al. (2017)) within the order *Tymovirales* (Figure 3B). Therefore, it was tentatively named *Armillaria ostoyae* RNA virus 1 (AoRV1, accession number OR670529) and likely placed within a monophyletic group as a potential new family along with other fungal and ant-associated RNA viruses.

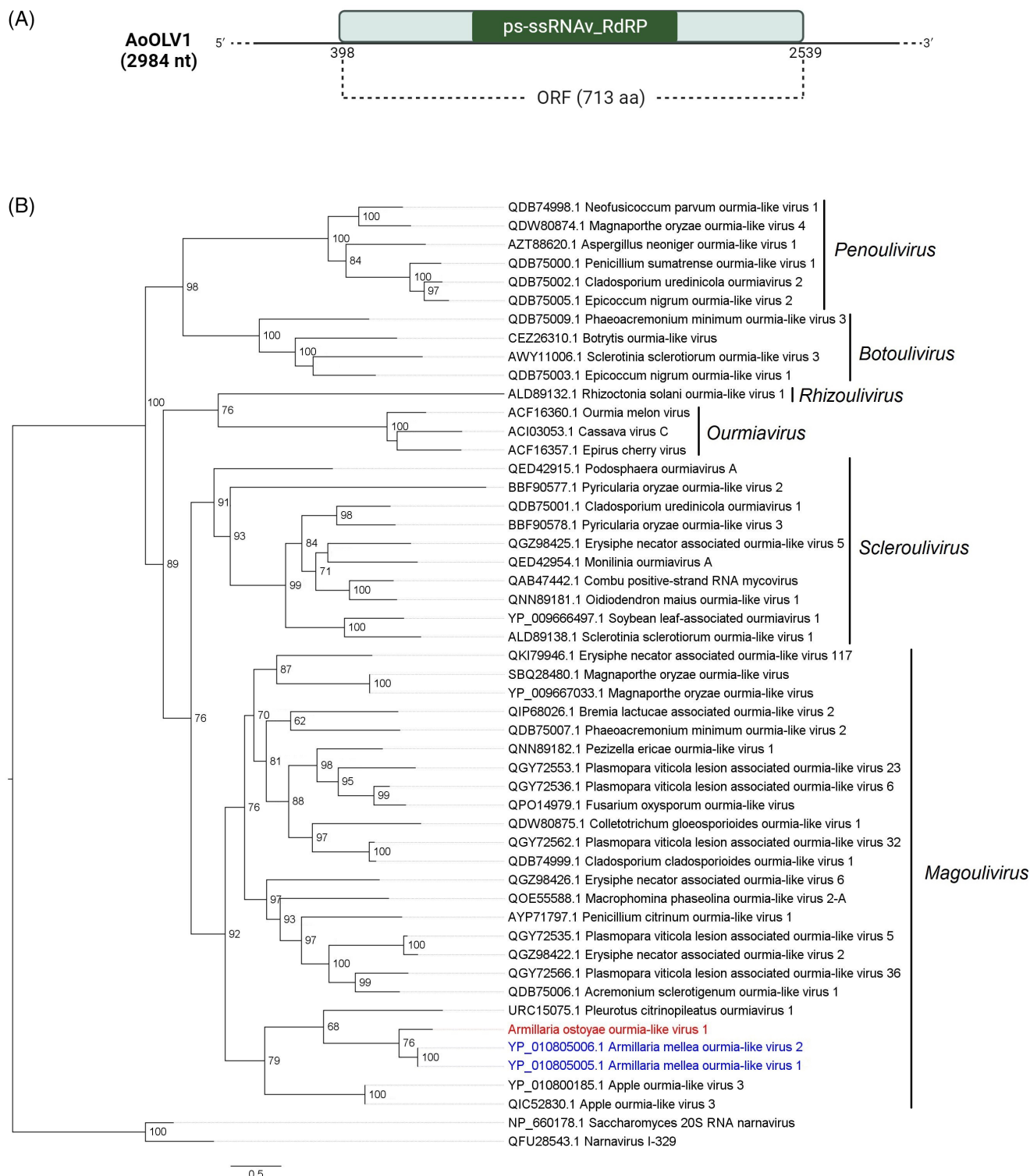


FIGURE 2 Genome organization and phylogeny of a novel ourmia-like virus from a French *A. ostoyae* isolate (M10666). (A) Schematic representation of AoOLV1 (+)ssRNA genome. The ORF is represented in green, with the RdRP domain in darker shading. (B) Maximum-likelihood phylogenetic tree of AoOLV1 with members of the family *Botourmiaviridae*. The tree was generated from the amino acid sequence alignment of the deduced RdRPs. The newly described virus is indicated in red and published virus variants also detected in this study are shown in blue. Two viruses (a yeast narnavirus, *Saccharomyces* 20S RNA narnavirus, and a narna-like virus, narnavirus I-329) are used as outgroups to root the tree. Numbers at nodes are bootstrap values out of 1000 replicates.

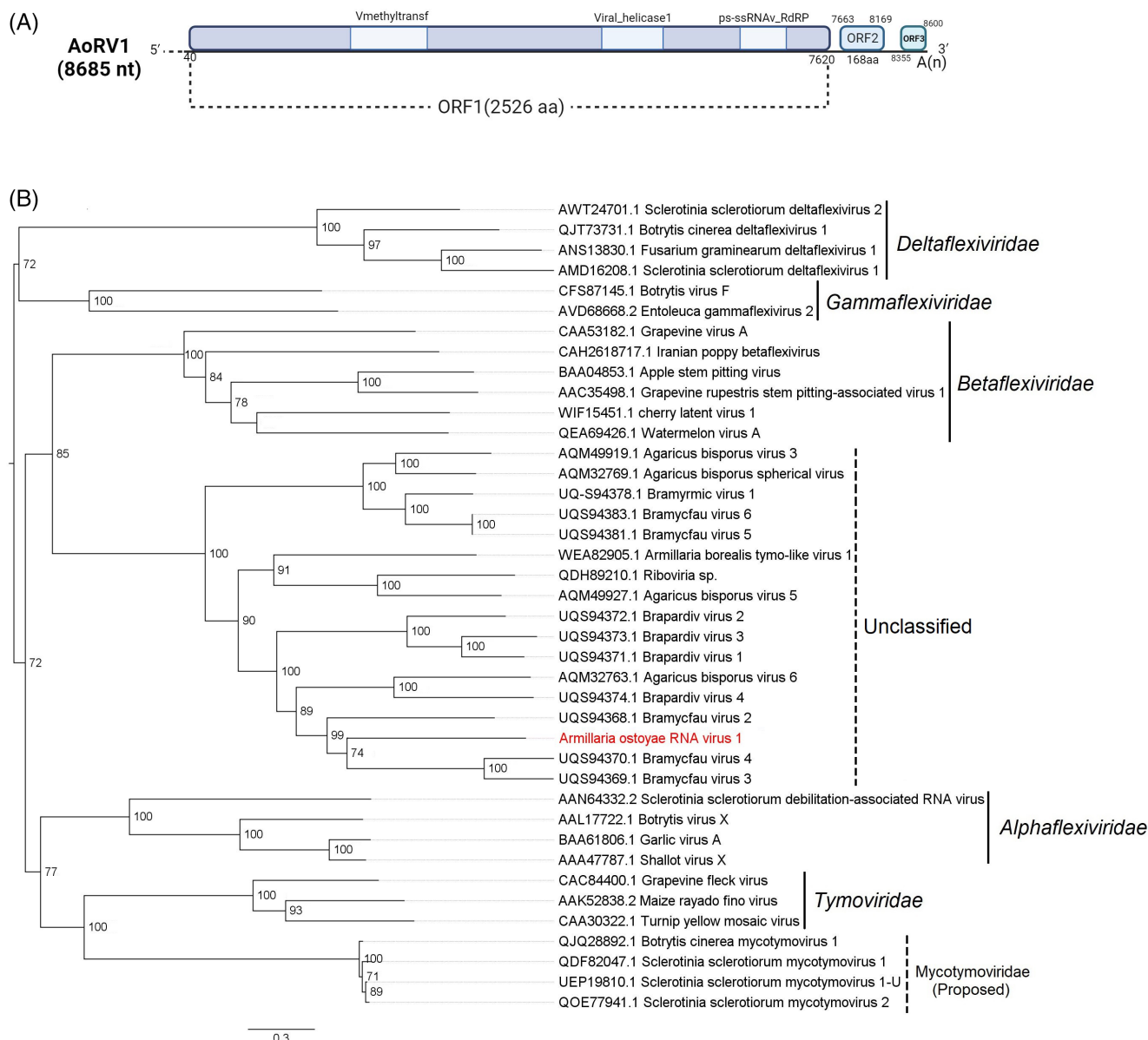


FIGURE 3 Genome organization and phylogeny of a novel ssRNA virus from *A. ostoyae* isolates. (A) Schematic representation of AoRV1 (+)ssRNA genome with predicted ORFs. The ORF1 is shown in blue and the three predicted conserved domains, methyltransferase, helicase, and RdRP, are shown with light shading. (B) Maximum-likelihood-based phylogenetic analysis of the ORF 1 protein of AoRV1 with closely related viruses selected members from five families (with two unassigned groups) in the order *Tymovirales*. The novel virus is shown in red. Numbers at nodes are bootstrap values out of 1000 replicates. Bootstrap values (%) <60 are not shown.

Mymonaviruses

Two virus-like contigs (Arm_P2-c408 and Arm_P3-c525), together with some other contigs associated with a known mymonavirus (*Armillaria mellea* negative-stranded RNA virus 1, AmNSRV1) (Linnakoski et al., 2021) were related to viruses of the family *Mymonaviridae* (Table 1). RT-PCR analysis showed a single Swiss *A. gallica* isolate (M10712) positive for Arm_P2-c408 and a single Swiss *A. cepistipes* isolate (M4393) positive for Arm_P3-c525 (Tables 2 and S1). These mymona-like viruses were named *Armillaria gallica* negative-stranded

RNA virus 1 (AgNSRV1, accession number OQ749610) and *Armillaria cepistipes* negative-stranded RNA virus 1 (AcNSRV1, accession number OR670530).

The complete genome of AgNSRV1 was 11,466 nt long and encoded one large ORF (ORF6; corresponding to Large (L) protein) of 1979 aa in length (222.2 kDa) and five small ORFs (see Figure 4A). The complete coding sequence of AcNSRV1 was 11,016 nt in length and it also encoded one large ORF (ORF6; corresponding to the L protein) of 1991 aa in length (221.5 kDa), five small ORFs upstream and a small ORF downstream the L protein (Figure 4A).

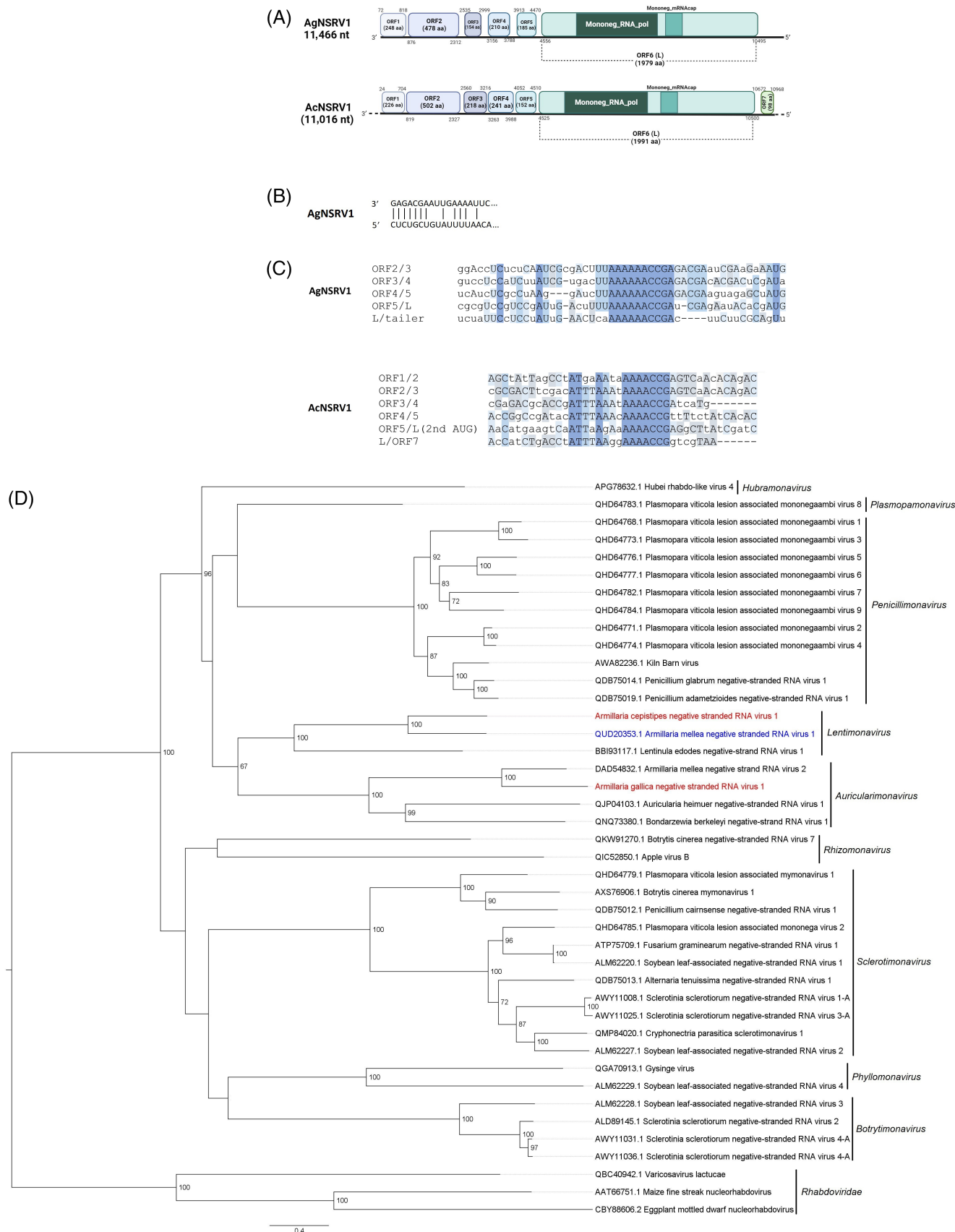


FIGURE 4 Legend on next page.

The BLASTp search of the L protein of AgNSRV1 and AcNSRV1 gave 53.2% identity with both *Armillaria mellea* negative-stranded RNA viruses AmNSRV1 and AmNSRV2, respectively (Table 1). The putative nucleoprotein (ORF2 protein) of AgNSRV1 and AcNSRV1 also shared moderate aa identities (39.5% and 43.6%, respectively) with the same viral counterparts (AmNSRV1 and 2; data not shown). Included in the L protein, a conserved domain for RNA polymerase (Mononeg_RNA_pol superfamily; cl15638) was detected at aa position 198–1017 and 221–1049 in AgNSRV1 and AcNSRV1, respectively. A second conserved domain for mRNA capping (Mononeg_mRNACap superfamily; cl16796) was found at aa positions 1073–1268 and 1106–1271 in AgNSRV1 and AcNSRV1, respectively. In AgNSRV1, terminal inverted complementarity, typical of mymonaviruses, was also observed for the 3'- and 5'-terminal nucleotides (Figure 4B). The putative gene-junction sequences were well conserved in each junction of AgNSRV1 (UUAAAAAACCGAgaCGA, well-conserved sequences show upper case letters), whereas those of AcNSRV1 were less conserved (AUuuAaaxAAAACCG) (Figure 4C). Phylogenetic analysis clustered AgNSRV1 and AcNSRV1 with members of the genus *Auricularimonavirus* and *Lentimonavirus*, respectively, in the family *Mymonaviridae* (Figure 4D) (Kuhn et al., 2021).

The species demarcation criteria for the members of the family *Mymonaviridae* have recently been updated: species in the genus differ by >30% in nucleoprotein amino acid sequence and by >30% in their complete coding sequence or complete genome nucleotide sequence (Jiāng et al., 2022). Our results suggest that AgNSRV1 and AcNSRV1 are novel members of the genera *Auricularimonavirus* and *Lentimonavirus*, respectively, in the family *Mymonaviridae*.

Partitivirus

Two contigs, possibly encoding two proteins that share sequence similarity with RdRP and the coat protein (CP) of known partitiviruses (Table 1) were identified. RT-PCR results indicated that only one *A. gallica* isolate (M10712) was positive for this virus. The complete sequences of the two genomic dsRNA segments were found to differ in size by 12 base pairs, the smaller one (dsRNA1; 1755 bp in length) corresponding to RdRP

and the larger one (dsRNA2; 1767 bp in length) corresponding to CP (Figure 5A). Generally, the sequence encoding for RdRP in partivirus is longer than the sequence encoding for CP, but exceptions have also been reported previously (Telengech et al., 2020).

The positive strands of both dsRNAs each encoded a single large ORF. ORF2 (dsRNA2) was 482 aa long (54 kDa) and ORF1 (dsRNA1) was 550 aa long (65 kDa) (Figure 5A), including a conserved domain for RdRP (RT_like superfamily; pfam cl02808) detected at aa position 239–391. BLASTp searches of the two polypeptides resulted in 21.6% and 65.6% aa sequence identities to the CP and RdRP of other alphapartitiviruses, respectively (Table 1). The RdRP-based ML phylogenetic tree placed the newly identified virus in the genus *Alphapartitivirus* (Figure 5B). At the 3' end of the dsRNA1, an interrupted poly (A) tail was present [(A)₁₇G(A)₇T(A)₅CG(A)₉], which is a characteristic of alphapartitiviruses. RdRP-based sequence alignment with other partitiviruses showed the presence of conserved motifs characteristic of partitiviruses (Figure S3a). Additionally, stem-loop structures were also predicted at the 5' termini of the two dsRNA segments (Figure S3b).

Based on these results and according to the ICTV species demarcation criteria for alphapartitiviruses (≤90% aa sequence RdRP identity and ≤80% aa sequence CP identity) (Vainio et al., 2018), the virus was considered a novel member of a new species in the genus *Alphapartitivirus* in the family *Partitiviridae* and was named *Armillaria gallica partitivirus 1* (AgPV1, accession numbers OQ749606 and OQ749607).

Unclassified dsRNA virus

A large virus-like contig of 10,700 nt was found to be similar to an unclassified dsRNA virus. In addition, at least 13 related virus-like contig fragments derived from variants of this dsRNA virus candidate were detected in other three pooled samples (pools P1, P2 and P4) with 93.3%–95.5% sequence identities (results not shown). RT-PCR analysis with primers based on the contig with the highest read count (Table S3) revealed that five fungal isolates were positive for this dsRNA virus, including species of *A. borealis*, *A. gallica* and *A. ostoyae* (Tables 2 and S1).

FIGURE 4 Genome organization and phylogeny of two novel mymonaviruses from Swiss isolates of *A. gallica* (M10712) and *A. cepistipes* (M4393). (A) Schematic representation of the AgNSRV1 and AcNSRV1 (–)ssRNA genomes with UTRs and predicted ORFs. The domains of RdRP and methyltransferase (guanine-N7-MTase) in L protein are also shown. (B) Complementarity in the 5'- and 3'-terminal sequences of the genomic RNA strand of AgNSRV1. (C) Alignment of the putative gene-junction sequences between ORFs in 3' to 5' orientation of AgNSRV1 and AcNSRV1. Conserved nucleotide sequences are highlighted in colour with the darkest colour indicating the highest conservation. (D) Maximum likelihood phylogenetic tree based on the L protein alignment with AgNSRV1, AcNSRV1 and selected members of nine genera of the family *Mymonaviridae*. The novel viruses are shown in red, and a previously published virus variant also detected in this study is shown in blue. Three plant rhabdoviruses (*Varicosvirus lactucae*, *Maize fine streak nucleorhabdovirus*, and *Eggplant mottled dwarf nucleorhabdovirus*) are used as outgroups. Numbers at nodes are bootstrap values out of 1000 replicates. Bootstrap values (%) <60 are not shown.

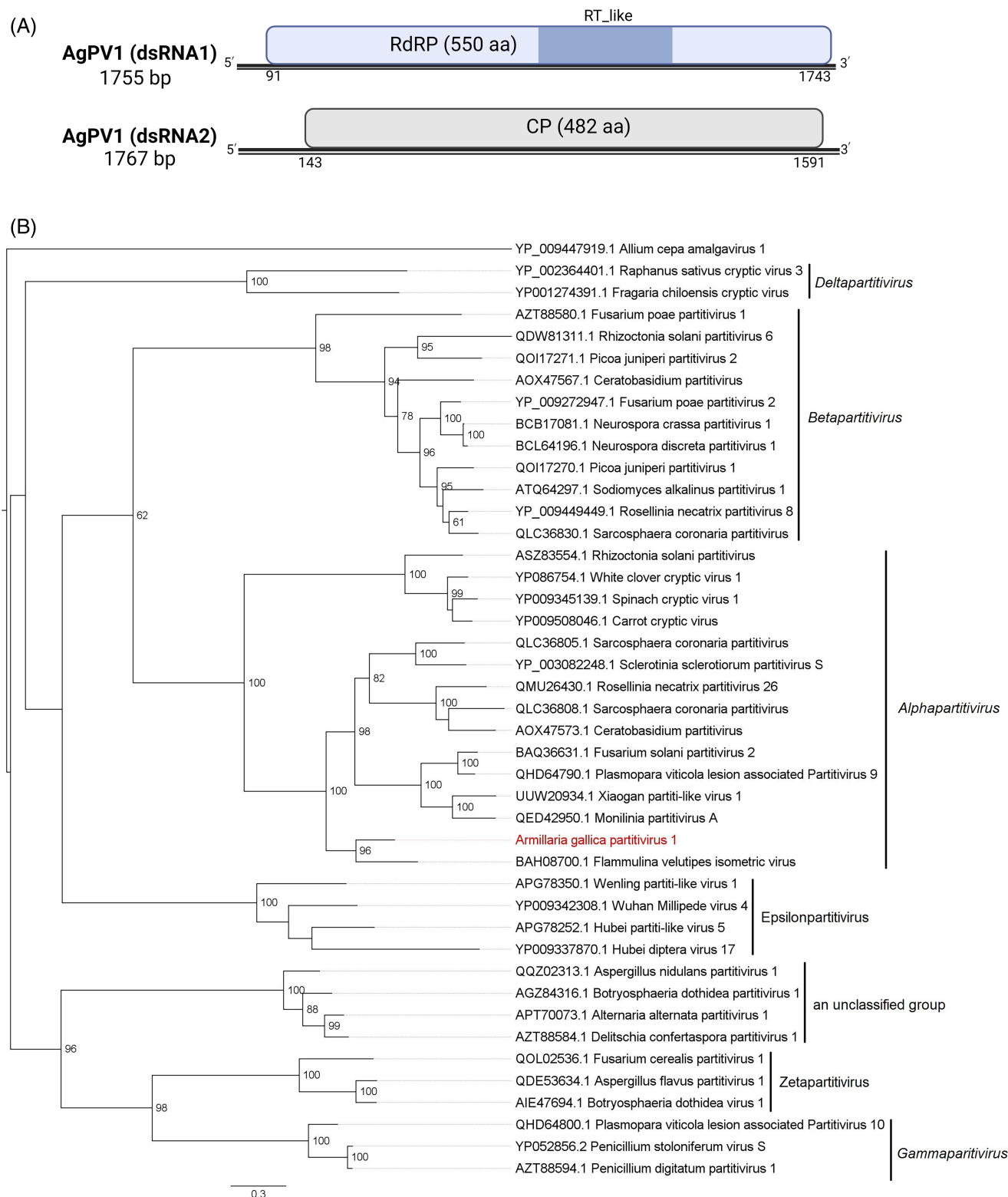


FIGURE 5 Genome organization and phylogeny of a novel partitivirus from a Swiss isolate of *A. gallica* (M10712). (A) Schematic representation of the AgPV1 genome with a bi-segmented dsRNA. The positive strand of the dsRNA1 encodes for RdRP. The dsRNA2 encodes for CP. The RdRP domain is shown in darker shading. (B) The maximum likelihood tree based on RdRP alignment with AgPV1 and selected members of six genera (with one unassigned group) of the family *Partitiviridae*. The novel virus is shown in red. *Allium cepa* amalgavirus 1 (family *Amalgaviridae*) is used as an outgroup to root the tree. Numbers at nodes are bootstrap values out of 1000 replicates. Bootstrap values (%) <60 are not shown.

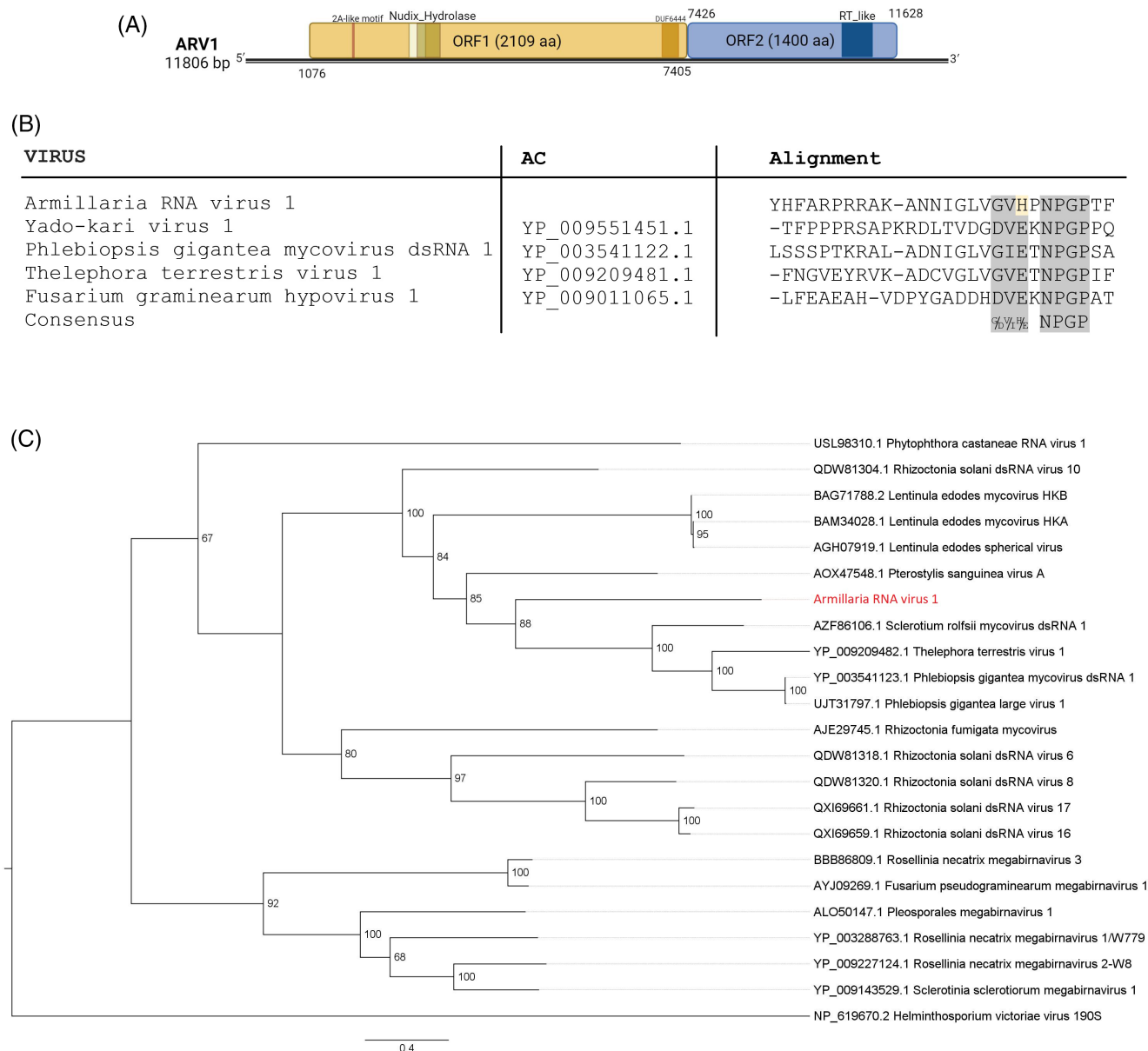


FIGURE 6 Genome organization and phylogeny of a novel dsRNA virus from *Armilaria* isolates. (A) Schematic representation of the ARV1 genome with UTRs predicted ORFs. The 2A-like motif, nudix hydrolase, and RdRp conserved domains are indicated by darker shaded boxes. (B) Comparison of the amino acid sequences around the 2A-like motifs in mycoviruses. The conserved residues are highlighted in grey. (C) The maximum likelihood tree based on the RdRP (ORF2 protein) alignment with ARV1 and related dsRNA viruses (phlegiviruses). The novel virus is shown in red. *Helminthosporium victoriae* virus 190S (family *Totiviridae*) is used as an outgroup. Numbers at nodes are bootstrap values out of 1000 replicates. Bootstrap values (%) <60 are not shown.

The complete dsRNA genome was found to be 11,806 bp long and its RdRP was similar to that of phlegiviruses in the proposed family ‘Phlegiviridae’ within the order *Ghabrivirales* (Sato et al., 2023) by BLASTp search (Table 1). Two non-overlapping ORFs were predicted in the positive strand of the dsRNA in different frames (Figure 6A). A stem-loop structure was predicted at the 5′ UTR (Figure S4b).

The 2109 aa long ORF1 (molecular weight 231.0 kDa) showed 27.3% identity to the RdRP of *Lentinula edodes* mycovirus HKB in BLASTp search (data not shown). Conserved domains for Nudix_Hydrolase

(Nudix_Hydrolase superfamily; cd02883 and cl00447) were found at aa positions 501–590 and 467–528, respectively, and a third domain (DUF6444 superfamily; cl45421) was present near the N-terminus of the ORF1 (aa position 2030–2107) (Figure 6A). In addition, a 2A-like self-processing peptide motif (G/DxExNPGP) predicted in some phlegiviruses (Petrzik et al., 2016) was also found in the N-terminal part of the ORF1 protein, but with a histidine residue (H) instead of the conserved glutamic acid (E, underlined) (Figure 6B).

The 1400 aa long ORF2 (molecular weight 158.4 kDa) exhibited 35.4% identity to RdRP of

Sclerotium rolfsii mycovirus and 36% identity to RdRP of *Phelebiopsis gigantea* large virus 1 in BLASTp search. The conserved domain for RdRP (RT_like superfamily; cl02808) was present at aa position 862–1046 (Figure 6A). All eight conserved motifs characteristic of the RdRP gene of dsRNA viruses were also found in the polypeptide encoded by ORF2 (Figure S4a). It can be speculated that a ribosomal –1 frameshift site is located upstream of the stop codon of ORF1, with a candidate sequence of ‘GGGUUUU’ instead of the known phlegivirus sequence ‘AAAAAAA’. The ‘GGGUUUU’ sequence was also predicted as a slippery site for red clover powdery mildew-associated totiviruses (dsRNA viruses, *Ghabri-virales*) (as described in Kondo et al. (2016)).

In ORF2-encoded protein-based phylogeny, the virus clustered with other unclassified dsRNA viruses belonging to the proposed family ‘Phlegiviridae’ (Figure 6C) (Sato et al., 2023). Based on the sequence analysis and phylogeny, the virus was considered a novel dsRNA virus in the new family together with several other mycoviruses, and was tentatively named *Armillaria* RNA virus 1 (ARV1, accession number OQ749611).

Ambiviruses

Ambiviruses were only recently described as circular ssRNA genomes with viroid-like self-cleaving elements (Forgia et al., 2023). Because the delineation criterion for ambiviruses has not yet been established, we have adhered to a threshold of 90% for the classification of new species, as recently proposed (Turina et al., 2023). Thus, contigs sharing more than 90% aa identity were considered variants of the same virus (results not shown). Consequently, 29 contigs were found to be variants of 10 different ambi-like viruses, which are described below (Table 1).

Based on the BLASTp analysis, two virus sequences were found to be variants of the ambi-like viruses, *Armillaria borealis* ambi-like viruses 2 (AbAIV2) and *Armillaria* sp. ambi-like virus 3 (AsALV3), previously described by Linnakoski et al., 2021 and one contig (Arm_P3-c40) was found to be a variant of an unpublished ambi-like virus, *Armillaria* spp. ambi-like virus 3 (AAIV3) (GenBank accession number WCL23002) (Table 1). Here we describe seven ambiviruses that have been classified as potential new viruses using BLASTp and protein identity (Figure S5a).

Among novel ambiviruses, four were prevalent across different fungal species and were named *Armillaria* spp. ambi-like virus 5–8 (AsAIV5–8, accession numbers OR670531, OR670538, OR670532 and OR670533), respectively (Tables 1 and 2). The remaining three novel ambi-like viruses were found exclusively in isolates of *A. mellea* and were therefore designated as *Armillaria mellea* ambi-like virus 3–5 (AmAIV3–5,

accession numbers OR670534 - OR670536), respectively (Tables 1 and 2). RT-PCR revealed infection frequencies between 1.2% and 16.9% depending on the *Armillaria* species (Table 2).

All seven described novel ambi-like viruses had a complete coding sequence, but AsAIV5 contained some ambiguous nucleotides (NNN) within the second ORF (ORF B) (Figure 7A). They were composed of bicistronic ambisense genomes encoding two major ORFs. Many of them also contain a third ORF with the same orientation (in the head-to-head interval region between two major ORFs), which is possibly conserved between viruses within each of the ambivirus families (data not shown), but its expression and function are still unknown (Linnakoski et al., 2021). Alignment of the ORF A-encoded polypeptides showed the presence of a conserved motif for RdRP (containing the GDD triplet) (Figure S5b). Phylogenetic analysis placed these viruses in one of the four proposed families (‘Dumbiviridae’, ‘Quambiviridae’, ‘Trimbiviridae’ and ‘Unambiviridae’, respectively) for ambiviruses and ambi-like viruses (Turina et al., 2023) (Figure 7B). *Armillaria* ambiviruses found outside the ‘Unambiviridae’ each formed a single clade within the family. In particular, up to 10 *Armillaria* ambivirus species were clustered in the clade within the ‘Dumbiviridae’. A similar topology of *Armillaria* viruses, but within the genus, was also found in the phylogenetic trees of mitovirids and mymonavirids, respectively (Figures 1D and 4D). Future studies may allow us to understand some aspects of the potential co-evolution of *Armillaria* and its viruses.

Viral occurrence and genetic diversity

Among the 166 screened isolates, 139 were carriers of at least one virus, which corresponds to a virus prevalence of 84.7% (Tables 2 and S1). However, only mitovirid, AbMV1, was very common (71.1%), while the other viruses were present in only 1–28 isolates (frequencies ranging from 0.6% to 16.9%) (Table 2). Viral diversity was highest in *A. mellea* with 10 different viruses, followed by *A. gallica* with 9 viruses, and *A. borealis*, *A. cepistipes* and *A. ostoyae* with 8 viruses each. Finally, the most common mitovirus AbMV1 was also detected in the two isolates of the closely related fungus *D. tabescens* (Table 2).

To verify the natural character of RNA-seq contigs that were found in different fungal isolates but in the same RNA-seq library, the RdRP coding region of 23 isolates that were PCR-positive for mitoviruses or ambi-like viruses was partially sequenced. The resulting consensus sequences were used for alignments together with the corresponding RNA-seq contig selected for genome characterization, and a pairwise comparison of sequences was calculated using CLC Main Workbench software. Except for AbMV1, pairwise comparisons showed that at least one of the Sanger

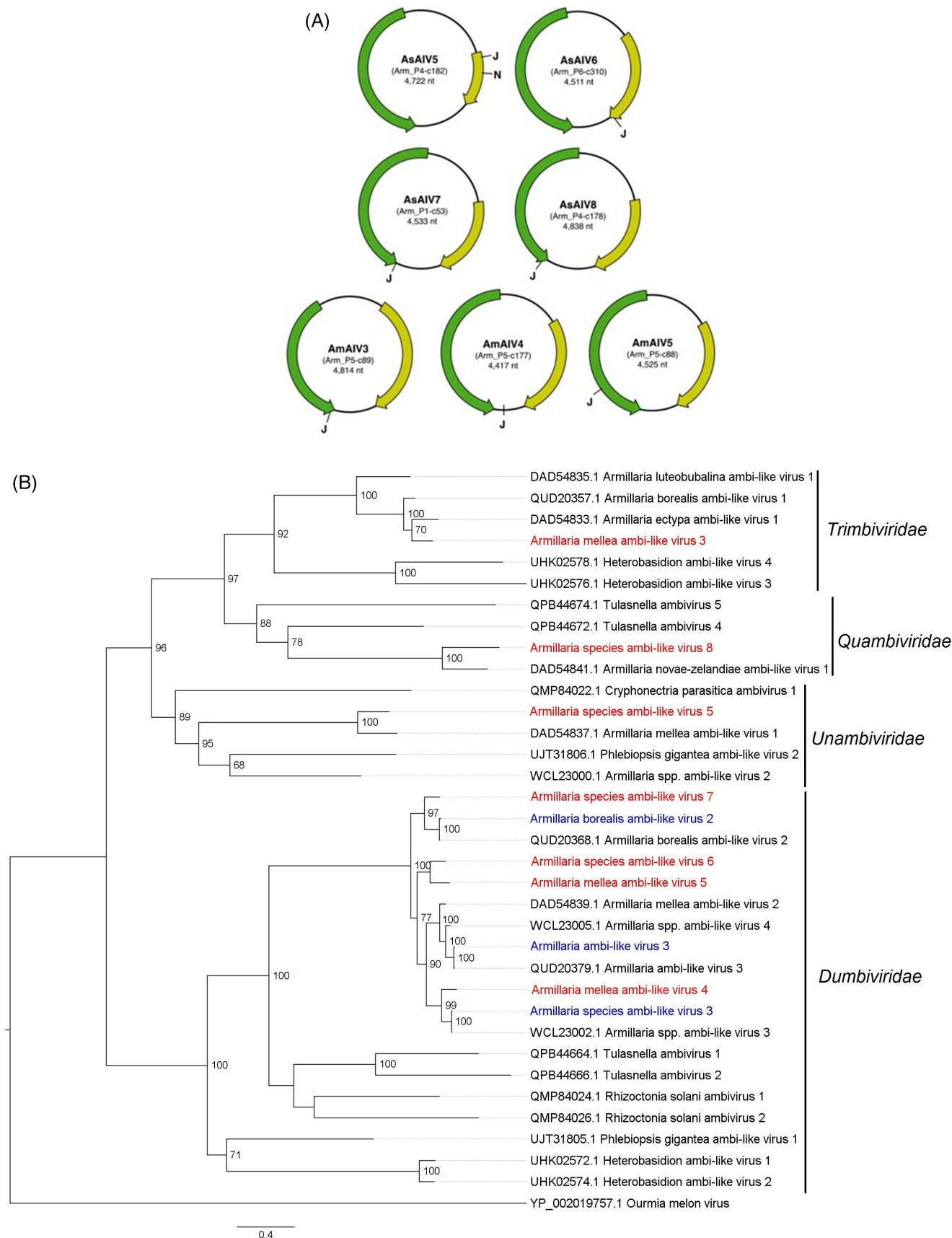


FIGURE 7 Legend on next page.

sequences was 100% identical to the RNA-seq contig used to characterize the viral genome, while others were with 88%–99% identity in the range of variants (Table 3, Figure S6a–g), demonstrating the natural character of the contig sequence and the presence of variants in different fungal species. Since the most similar Sanger sequence to the AbMV1 contig had only 98.77% identity (Figure S6a), additional contigs overlapping with the Sanger sequenced region were included in the pairwise comparison. The results show that several Sanger sequences of AbMV1 detected in *A. borealis*, *A. ostoyae*, *A. mellea* and *D. tabescens* were 100% identical with different RNA-seq contigs (Figure S6a). Other viruses were not analysed as they were only found in a single isolate per RNA-seq pool.

Viral co-infections

Due to the high frequency of a mitovirus (AbMV1) and the high number of ambi-like viruses, viral co-infections were numerous and combined in a variety of ways (Table S4). At least 34.9% of all isolates were infected with two or more viruses. In *A. cepistipes* viral co-

infections reached a frequency of 82.4%, followed by *A. mellea* with 73.7%, whereas in *A. borealis*, *A. gallica* and *A. ostoyae* the viral co-infection rate ranged between 7.5% and 35.0%. Two Swiss isolates of *A. mellea* (M9597 and M9601) were found to be co-infected with seven different viruses. In addition, AMV1 was found in co-infections with all other viruses except AoOIV1 and AoRV1. Interestingly, although a large number of *A. ostoyae* isolates were infected with viruses (73.1%), the majority of isolates were infected with a single virus (65.7%). In contrast, the majority of *A. mellea* isolates were infected with two or more viruses (73.7%) and only nine of 38 (23.7%) contained a single virus (Figure 8).

Host range and geographic distribution of viruses

Of the 21 viruses detected, 16 occurred in more than one fungal isolate: six were host-specific and detected in only one *Armillaria* species, and 10 exhibited a broad fungal host range, infecting two to six different species (Tables 2 and S1). The highly frequent mitovirus

TABLE 3 Pairwise comparison, amplicon length and GenBank accession number of Sanger sequences of the RdRP coding region of selected mito- and ambi-viruses.

Virus/reference contig (GB accession)	<i>A. borealis</i>	<i>A. cepistipes</i>	<i>A. gallica</i>	<i>A. mellea</i>	<i>A. ostoyae</i>	<i>D. tabescens</i>	Amplicon length [nu]	GenBank no.
AbMV1 ^a /Arm_P5-c38 (OQ749608)	98.77	93.65–93.83	94.36	88.71–93.83	89.77–95.41	93.83	567	OR983282–OR983287
AMV1/Arm_P1-c69 (OQ749609)	100	94.41	94.68	n.a.	92.29	n.a.	376	OR983288–OR983291
AsAIV5/Arm_P4-c182 (OR670531)	n.a.	94.51	100	94.51	n.a.	n.a.	437	PP002097–PP002099
AsAIV6/Arm_P6-c310 (OR670532)	95.93	n.a.	n.a.	100	n.a.	n.a.	540	PP002100, PP002101
AsAIV7/Arm_P1-c53 (OR670533)	100	n.a.	n.a.	89.88	90.38	n.a.	603	PP002106–PP002108
AsAIV8/Arm_P4-c178 (OR670534)	100	n.a.	100	n.a.	n.a.	n.a.	468	PP002109, PP002110
AsAIV3 ^a /Arm_P4-c50 (OR670537)	94.69	99.82	n.a.	n.a.	88.32	n.a.	565	PP002102–PP002105

Note: Shown is the identity (%) of the viral reference contigs compared with the Sanger sequences. One value represents the comparison of the reference contig with one Sanger sequence, one identity range represents the comparison of the reference contig with one Sanger sequence and additional contigs (see Figure S6 for details).

^aVariants of viruses previously reported by Linnakoski et al. (2021) or deposited in GenBank.

FIGURE 7 Genome organization and phylogeny of novel ssRNA viruses from *Armillaria* species. (A) Schematic representation of putative circular ssRNA genomes of novel ambi-like viruses, including both largest ORFs found using NCBI's ORF Finder program. The arrows represent the strand polarity of bicistronic, ambisense genomes, and the colours indicate ORF A (green) and ORF B (yellow). The letter J stands for the junction, the site of the contig where the sequence was interrupted, and N for a short ambiguous region (NNN) in the contig of AsAIV5. (B) Maximum likelihood tree of the RdRP (ORF1 protein) alignment of *Armillaria* ambi-like viruses and other related viruses (four proposed families). The novel viruses are highlighted in red and previously published viral variants, which were also detected in this study, are coloured in blue. Ourmia melon virus (a plant ssRNA virus, family *Botourmiaviridae*) is used as an outgroup. Numbers at nodes are bootstrap values out of 1000 replicates. Bootstrap values (%) <60 are not shown.

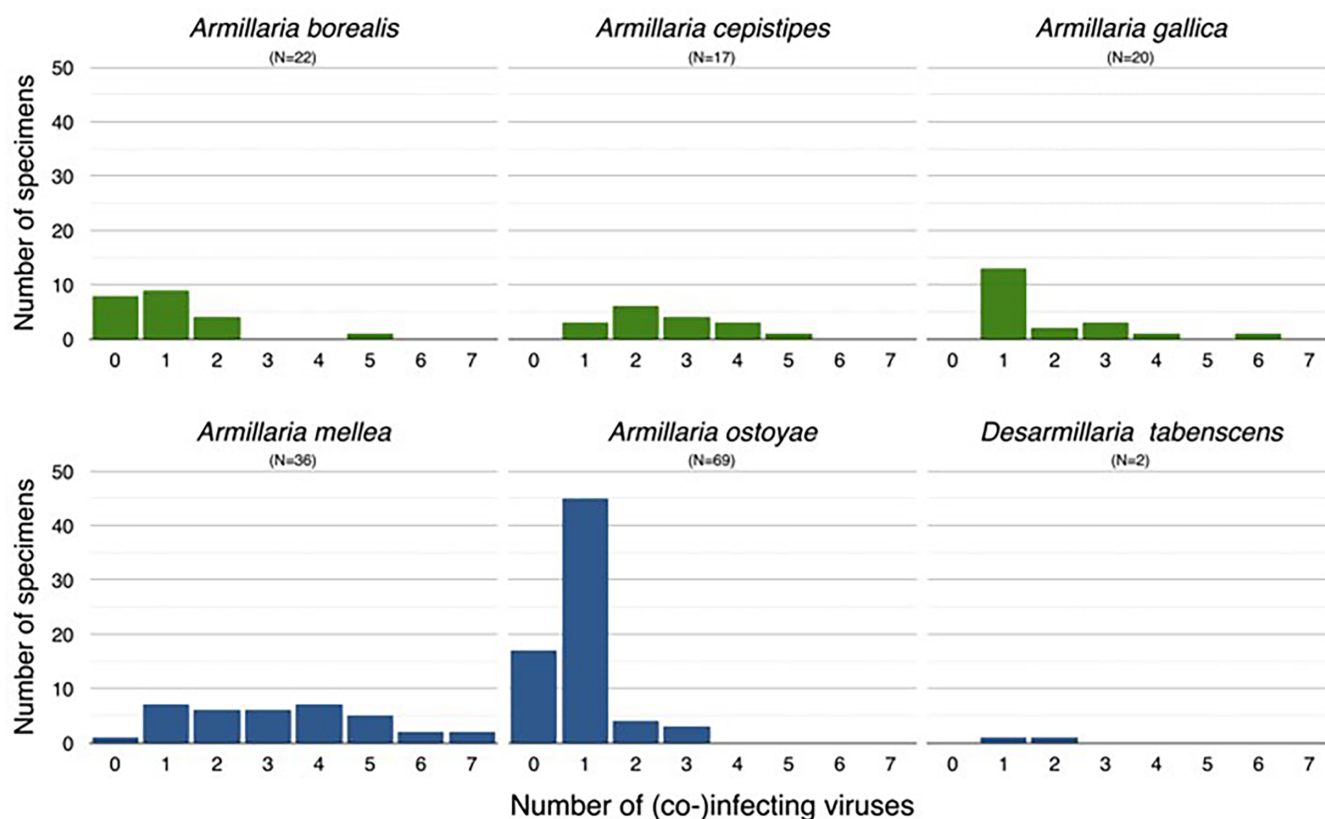


FIGURE 8 Number of viruses (0–7) detected per isolate among the assessed *Armillaria* or *Desarmillaria* species. Further details about co-infecting viruses are provided in Table S4; 0 or 1 represents the number of samples in which no or only one virus was detected.

AbMV1 was present in all tested *Armillaria* species as well as in *D. tabescens*. This virus was also geographically most widespread and was detected in isolates from Switzerland and from all neighbouring countries and Spain (Tables S1 and S5). The other 15 viruses with multiple occurrences were all detected in Switzerland, and seven of them also in one or several neighbouring countries. All viral species with multiple occurrences were detected in more than one sampling year, with detection periods ranging from 6 to at least 33 years. The viruses with single occurrences were either sampled in Switzerland or France (Table S5).

Correlation of the virus presence and the virulence of *Armillaria*

An important objective of this study was to evaluate whether mycoviruses might be involved in the virulence gradient among the species/ isolates previously tested in subsets of *A. borealis*, *A. cepistipes*, *A. mellea* and *A. ostoyae*. However, no clear effect of viruses on virulence between or within *Armillaria* species was detected (Table S2). The viral co-infection load (i.e., the cumulative number of viral species present in a fungal isolate) did not correlate with the fungal species pathogenicity, that is, a high viral co-infection load was

observed for both the primary pathogen *A. mellea* and the secondary pathogen/saprotroph *A. cepistipes*. Conversely, the primary pathogen *A. ostoyae* and the secondary pathogen *A. borealis* were found to have a low viral co-infection load compared with the other *Armillaria* species tested in this study. Within species, the presence or absence of viruses was not correlated with the virulence ranking (Table S2).

From the current data, it is difficult to draw conclusions about the effect of individual viral species on the virulence of fungal hosts, because either many viral co-infections were observed or viruses occurred too rarely. In *A. ostoyae* alone, AbMV1 was shown to have no effect on virulence, as this virus occurred without coinfection in 7 isolates covering the whole virulence spectrum.

DISCUSSION

Armillaria hosts both ss- and dsRNA viruses, with a mitovirus being the most frequent

In the present study, 21 different mycoviruses were found among 166 isolates of five *Armillaria* and one *Desarmillaria* species, including 14 novel viruses with ssRNA and dsRNA genomes. Based on their full-length

or complete-coding genomes and aa sequences, these viruses represent putative new species within four established families (*Partiti*-, *Mito*-, *Botourmia*-, *Mymonaviridae*) or a proposed family ('*Phlegiviridae*'), and within four ambiviral proposed families (order '*Crytulvirales*'). Another new virus appears to be an unclassified ssRNA virus (unclassified *Tymovirales*), while the remaining viruses are variants of previously reported or deposited ssRNA viruses (*Mito*-, *Botourmia*-, *Mymonaviridae* and '*Dumbiviridae*') or ambi-like viruses (Linnakoski et al., 2021).

Additionally, this study reports for the first time the occurrence of two dsRNA viruses (a partitivirus and a phlegivirus) in the basidiomycete genus *Armillaria*. Previous attempts to detect the presence of dsRNA elements in 40 isolates of three different *Armillaria* species (*A. gallica*, *A. cepistipes* and *A. ostoyae*) from the Czech Republic as well as in 63 isolates of the same three species plus *A. borealis* from Finland, Russia and South Africa were unsuccessful probably due to methodological reasons (Dvořák, 2008; Linnakoski et al., 2021). In line with these results, the two dsRNA viruses, AgPV1 (1 occurrence) and ARV1 (5 occurrences), detected in this study were rare and restricted to isolates from Switzerland. Nevertheless, one of the dsRNA viruses (ARV1) was present in three different *Armillaria* species.

An unclassified virus of *Tymovirales* (AoRV1) is reported here for the first time for the genus *Armillaria*. The existence of mitoviruses in *Armillaria* species has recently been demonstrated by several laboratories with a variant of AbMV1 (accession number ON875998, unpublished) deposited in GenBank and an AMV1-related sequence (OR349296) recently published (Erkmen et al., 2023). AbMV1 was the most (71.1%) prevalent virus in our collection, it was not detected in the study of Linnakoski et al. (2021), nor was the rather rare virus from *Tymovirales*. In addition, a variant of an unpublished ambi-like virus (AAIV3) released in GenBank (ON380552) was found to be above the recently proposed threshold of 90% similarity and thus represent the same virus. We have here for the first time described the occurrence of these viruses in different *Armillaria* species and *D. tabescens* and their distributions in European *Armillaria* populations.

In this study, we report the frequency of 21 different viruses in 166 fungal isolates analysed by RT-PCR. However, an important limitation of this frequency analysis is the fact that the RT-PCR primers were designed based on one or a few contigs of each virus. Therefore, our RT-PCR screening may contain false-negative results because some viral variants were not amplified due to nucleotide polymorphism in the primer sequence. For this reason, we assume that the frequencies and host range presented here underestimate the actual viral occurrence in our sample.

Viral co-infections are common in *Armillaria*

Co-infection by multiple viruses is a common phenomenon in fungi (Bartholomäus et al., 2016; Osaki et al., 2016). Co-infection can result in complex interplay between viruses resulting either in mutualism, synergism, antagonism, or genomic rearrangements (Chiba & Suzuki, 2015; Sasaki et al., 2016; Sun et al., 2006; Sun & Suzuki, 2008; Yang et al., 2021). In Basidiomycetes, viral co-infection has been reported in isolates of *Armillaria* spp. (Linnakoski et al., 2021), *Heterobasidion* spp. (Hantula et al., 2020; Kashif et al., 2015; Vainio et al., 2015), *Agaricus bisporus* (Romaine & Schlagnhauser, 1995), *Lentinula edodes* (Guo et al., 2017) and *Bondarzewia berkleyi* (Vainio & Sutela, 2020).

In the present study, we found mixed infections in all *Armillaria* species examined (Figure 8, Table S4), and in about one-third of all isolates (34.9%), including two Swiss isolates of *A. mellea* (M9597 and M9601) that were co-infected with seven different viruses (Figure 8). Remarkable is the even distribution of co-infections in *A. cepistipes*, *A. gallica* and *A. mellea* compared with the sister species *A. borealis* and *A. ostoyae*, which were rarely infected by viruses and if so, mostly by one virus. The analysis of such co-infections is interesting, but also challenging because it is difficult to generate isogenic, virus-free fungal isolates with which to perform Koch's postulates for each virus. Although Linnakoski et al. (2021) were successful in producing isogenic virus-free lines following heat treatment, in the case of our isolates, the high number of virus co-infections and the high frequency of mitoviruses present a particular hurdle as they reside in mitochondria.

Armillaria viruses persist over decades or even centuries

An interesting finding of this study is the detection of viruses with high sequence identity with the previously described mymonavirus AmNSRV1 and the ourmia-like virus AmOIV2 in *A. mellea* isolates from Switzerland. Both viruses were initially discovered in *A. mellea* isolates from Cape Town, South Africa (Linnakoski et al., 2021). A previous study has hypothesized that *A. mellea* was introduced into South Africa in the mid-1600s by Dutch settlers with potted plants from Europe (Coetzee et al., 2001). However, the actual introduction event in Cape Town is not documented, and the scientifically proven history only goes back to the last century. The European origin of the South African *A. mellea* isolates was verified by phylogenetic analyses that placed them in the European clade of *A. mellea*, which is distinct from the Asian and North American clades. The fact that the same two viruses,

AmNSRV1 and AmOIV2, were found in European and South African *A. mellea* isolates strongly supports the European origin of *A. mellea* in Cape Town. This also suggests that these two viruses were already circulating in the European population of *A. mellea* at least since the last century and have persisted in both the South African and European populations since then.

Direct evidence that *Armillaria* viruses can circulate in populations for at least several decades is provided by 10 viruses described in this study whose detection periods ranged between 20 and at least 33 years (Table S5). Similarly, the Cryphonectria hypovirus 1 (genus *Hypoviridae*), hosted by the ascomycete fungus *Cryphonectria parasitica*, has been detected in isolates collected over four decades (Bryner et al., 2012). This study was limited to the occurrence of viruses in isolates collected over the past 40 years and preserved in our institute culture collection at WSL. It was therefore not possible to assess the long-term persistence of single viral variants in relation to host or geography. Further research on the genetic diversity of viruses within and between host species is needed to better understand viral gene flow in *Armillaria* populations as a function of geography and host over time.

Signal of cross-species virus transmission and no correlation with virulence

The two mitoviruses, the unclassified dsRNA virus, and the ambi-like viruses were hosted by more than one *Armillaria* species. The most frequent virus, AbMV1, was detected in all five *Armillaria* species examined as well as in *D. tabescens*, from the sister genus *Desarmillaria* recently split from the genus *Armillaria*. Linnakoski et al. (2021) also reported an ambi-like virus in two different *Armillaria* species. All in all, these findings suggest that these viruses can cross species boundaries and may occasionally be transmitted between both, closely and more distantly related *Armillaria* species. A recently published genome analysis supports the idea of horizontal transfer of genetic material between different fungal species. This study shows that *Armillaria* fungi have acquired a considerable number of genes mainly from Ascomycetes by horizontal gene transfer (Sahu et al., 2023). Interestingly, all viruses present in multiple species appear to be transmitted between closely but also more distantly related species, as none of these viruses were restricted to sister species *A. cepistipes*—*A. gallica* or *A. borealis*—*A. ostoyae* (Koch et al., 2017; Tsykun et al., 2013).

Sympatric occurrence of closely and more distantly related *Armillaria* species in the same forest stand and spatial overlap of different species are regularly observed (Bendel, Kienast, & Rigling, 2006; Dalya et al., 2019; Legrand et al., 1996; Prospero, Rigling, &

Holdenrieder, 2003; Warwell et al., 2019). Additionally, *Armillaria* individuals can reach considerable age and size (Bendel, Kienast, & Rigling, 2006; Ferguson et al., 2003; Smith et al., 1992), increasing the likelihood that individuals of the same or different species interact. In another root rot pathogen, *Heterobasidion* spp., virus exchange between clones of the same species and across species boundaries is well documented and experimentally verified (Ihrmark et al., 2002; Vainio et al., 2011; Vainio et al., 2015).

Interestingly, the viruses described in the present study are also related to viruses reported from other basidiomycetes that are root rot pathogens or saprotrophs and inhabit a similar ecological niche as *Armillaria*. For example, a closely related virus of AbMV1 is a mitovirus of the root rot pathogen *Heterobasidion annosum* (Vainio, 2019). Fungi of the genus *Heterobasidion* are widespread in coniferous forests in the Northern Hemisphere and frequently co-occur with *Armillaria* (e.g., Bendel, Kienast, Bugmann, & Rigling, 2006; Dalya et al., 2019). Findings of previous studies support the occasional transfer of viruses between fungal species sharing the same habitat (Arjona-Lopez et al., 2018; Vainio et al., 2017; Yaegashi & Kanematsu, 2016). Future studies are needed that screen different *Armillaria* species and other sympatric basidiomycetes from the same forest stand to test the hypothesis of occasional cross-species virus transmission in soil-borne fungal pathogens.

Finally, the viral infection rate of the *Armillaria* isolates did not correlate with the virulence classification of previously tested subsets of *A. borealis*, *A. cepistipes*, *A. mellea* and *A. ostoyae*. Viruses and co-infecting viral species were present (or absent) in isolates across the entire virulence spectrum. In *A. ostoyae*, AbMV1 was, with one exception, the only virus present among isolates examined for virulence, and it was found in both high- and low-virulence isolates, suggesting that it has more of a neutral effect on host virulence in this *Armillaria* species. To gain a deeper understanding of how the viruses outlined in this study affect the virulence of their hosts, additional experiments comparing the virulence of isogenic isolates with and without the virus would be required. Since we observed frequent viral co-infections, it will also be interesting to investigate the cumulative effects of different viral combinations.

AUTHOR CONTRIBUTIONS

Wajeaha Shamsi: Funding acquisition; formal analysis; investigation; methodology; visualization; writing – original draft. **Renate Heinzelmann:** Funding acquisition; methodology; resources; writing – review and editing. **Sven Ulrich:** Methodology; validation. **Hideki Kondo:** Data curation; formal analysis; software; writing – review and editing. **Carolina Cornejo:** Conceptualization; funding acquisition; project administration; supervision; writing – review and editing.

ACKNOWLEDGEMENTS

We thank Daniel Rigling and Simone Prospero for their generous support at all stages of this study. We also thank Valentin Queloz for making his *Armillaria* collection available for this study. This work was funded by the WSL internal grant no. 202111N2343 to CC, RH and WS, and also supported by the Swiss Federal Institute for Forest, Snow and Landscape Research. Open access funding provided by ETH-Bereich Forschungsanstalten.


CONFLICT OF INTEREST STATEMENT

The authors declare no conflict of interest.

DATA AVAILABILITY STATEMENT

The sequence data are publicly accessible in the NCBI database under the BioProject accession number PRJNA1017781: <https://www.ncbi.nlm.nih.gov/bioproject/PRJNA1017781>. The amplicon sequences of mitoviruses, accessions OR983282-OR983291, and ambiviruses, accessions PP002097-PP002110.


ORCID

Wajeeha Shamsi  <https://orcid.org/0000-0002-9628-5885>

Renate Heinzelmänn  <https://orcid.org/0009-0004-4599-8430>

Sven Ulrich  <https://orcid.org/0009-0009-2042-8331>

Hideki Kondo  <https://orcid.org/0000-0001-9220-5350>

Carolina Cornejo  <https://orcid.org/0000-0003-3259-6198>

REFERENCES

- Ahn, I.-P. & Lee, Y.H. (2001) A viral double-stranded RNA up-regulates the fungal virulence of *Nectria radicola*. *Molecular Plant-Microbe Interactions*, 14, 496–507.
- Anthony, M.A., Bender, S.F. & van der Heijden, M.G.A. (2023) Enumerating soil biodiversity. *Proceedings of the National Academy of Sciences*, 120, e2304663120.
- Arjona-Lopez, J.M., Telengech, P., Jamal, A., Hisano, S., Kondo, H., Yelin, M.D. et al. (2018) Novel, diverse RNA viruses from Mediterranean isolates of the phytopathogenic fungus, *Rosellinia necatrix*: insights into the evolutionary biology of fungal viruses. *Environmental Microbiology*, 20, 1464–1483.
- Ayllón, M.A., Turina, M., Xie, J., Nerva, L., Marzano, S.-Y.L., Donaire, L. et al. (2020) ICTV virus taxonomy profile: *Botourmiaviridae*. *Journal of General Virology*, 101, 454–455.
- Bartholomäus, A., Wibberg, D., Winkler, A., Pühler, A., Schlüter, A. & Varrelmann, M. (2016) Deep sequencing analysis reveals the mycoviral diversity of the virome of an avirulent isolate of *Rhizoctonia solani* AG-2-2 IV. *PLoS One*, 11, e0165965.
- Baumgartner, K., Coetzee, M.P. & Hoffmeister, D. (2011) Secrets of the subterranean pathosystem of *Armillaria*. *Molecular Plant Pathology*, 12, 515–534.
- Bendel, M., Kienast, F., Bugmann, H. & Rigling, D. (2006) Incidence and distribution of *Heterobasidion* and *Armillaria* and their influence on canopy gap formation in unmanaged mountain pine forests in the Swiss Alps. *European Journal of Plant Pathology*, 116, 85–93.
- Bendel, M., Kienast, F. & Rigling, D. (2006) Genetic population structure of three *Armillaria* species at the landscape scale: a case study from Swiss Pinus mugo forests. *Mycological Research*, 110, 705–712.
- Botella, L., Janoušek, J., Maia, C., Jung, M.H., Raco, M. & Jung, T. (2020) Marine oomycetes of the genus *Halophytophthora* harbor viruses related to bunyaviruses. *Frontiers in Microbiology*, 11, 1467.
- Botella, L., Manny, A., Nibert, M. & Vainio, E.J. (2021) Create 100 new species and four new genera (Cryppavirales: Mitoviridae). ICTV 2021 proposal. https://ictv.global/taxonomy/taxondetails?taxnode_id=202213794&taxon_name=Duamitovirusalal1
- Bryner, S.F., Rigling, D. & Brunner, P.C. (2012) Invasion history and demographic pattern of Cryphonectria hypovirus 1 across European populations of the chestnut blight fungus. *Ecology and Evolution*, 2, 3227–3241.
- Chiba, S. & Suzuki, N. (2015) Highly activated RNA silencing via strong induction of dicer by one virus can interfere with the replication of an unrelated virus. *Proceedings of the National Academy of Sciences of the United States of America*, 112, E4911–E4918.
- Coetzee, M.P., Wingfield, B.D., Harrington, T.C., Steimel, J., Coutinho, T.A. & Wingfield, M.J. (2001) The root rot fungus *Armillaria mellea* introduced into South Africa by early Dutch settlers. *Molecular Ecology*, 10, 387–396.
- Cromey, M.G., Drakulic, J., Beal, E.J., Waghorn, I.A.G., Perry, J.N. & Clover, G.R.G. (2020) Susceptibility of garden trees and shrubs to *Armillaria* root rot. *Plant Disease*, 104, 483–492.
- Dalya, L., Capretti, P., Ghelardini, L. & Jankovsky, L. (2019) Assessment of presence and distribution of *Armillaria* and *Heterobasidion* root rot fungi in the forest of Vallombrosa (Apennines Mountains, Italy) after severe windstorm damage. *iForest – Biogeosciences and Forestry*, 12, 118–124.
- Deakin, G., Dobbs, E., Bennett, J.M., Jones, I.M., Grogan, H.M. & Burton, K.S. (2017) Multiple viral infections in *Agaricus bisporus* - characterisation of 18 unique RNA viruses and 8 ORFs identified by deep sequencing. *Scientific Reports*, 7, 2469.
- Dvořák, J. (2008) Diplomova práce. Univerzita Karlova, Přírodovědecká fakulta, Katedra genetiky a mikrobiologie. RNA elements in the genus *Armillaria*. Diploma thesis (2008) [In Czech]. <http://hdl.handle.net/20.500.11956/1281>
- Enderle, R., Sander, F. & Metzler, B. (2017) Temporal development of collar necroses and butt rot in association with ash dieback. *iForest – Biogeosciences and Forestry*, 10, 529–536.
- Erkmen, S., Sahin, E. & Akata, I. (2023) Full-length genome characterization of a novel mitovirus isolated from the root rot fungus *Armillaria mellea*. *Virus Genes*. <https://doi.org/10.1007/s11262-023-02041-8>
- Ezawa, T., Silvestri, A., Maruyama, H., Tawaraya, K., Suzuki, M., Duan, Y. et al. (2023) Structurally distinct mitoviruses: are they an ancestral lineage of the Mitoviridae exclusive to arbuscular mycorrhizal fungi (Glomeromycotina)? *mBio*, 14, e00240-23.
- Ferguson, B.A., Dreisbach, T.A., Parks, C.G., Filip, G.M. & Schmitt, C.L. (2003) Coarse-scale population structure of pathogenic *Armillaria* species in a mixed-conifer forest in the Blue Mountains of northeast Oregon. *Canadian Journal of Forest Research*, 33, 612–623.
- Forgia, M., Navarro, B., Daghighi, S., Cervera, A., Gisela, A., Perotto, S. et al. (2023) Hybrids of RNA viruses and viroid-like elements replicate in fungi. *Nature Communications*, 14, 2591.
- Fuke, K., Takeshita, K., Aoki, N., Fukuhara, T., Egusa, M., Kodama, M. et al. (2011) The presence of double-stranded RNAs in *Alternaria alternata* Japanese pear pathotype is associated with morphological changes. *Journal of General Plant Pathology*, 77, 248–252.
- Ghabrial, S.A., Castón, J.R., Jiang, D., Nibert, M.L. & Suzuki, N. (2015) 50-plus years of fungal viruses. *Virology*, 479–480, 356–368.

- Gross, A., Holdenrieder, O., Pautasso, M., Queloz, V. & Sieber, T.N. (2014) *Hymenoscyphus pseudoalbidus*, the causal agent of European ash dieback. *Molecular Plant Pathology*, 15, 5–21.
- Guillaumin, J.-J., Mohammed, C., Anselmi, N., Courtecuisse, R., Gregory, S.C., Holdenrieder, O. et al. (1993) Geographical distribution and ecology of the *Armillaria* species in western Europe. *European Journal of Forest Pathology*, 23, 321–341.
- Guillaumin, J.J., Mohammed, C. & Berthelay, S. (1989) *Armillaria* species in the northern temperate hemisphere. In: Morrison, D.J. (Ed.) *Proceedings of the 7th international conference on root and butt rots, Victoria and Vernon, British Columbia, Canada, 9–16 August 1988*. Forestry Canada: International Union of Forestry Research Organisations Working Party S2.06.01.
- Guindon, S., Dufayard, J.-F., Lefort, V., Anisimova, M., Hordijk, W. & Gascuel, O. (2010) New algorithms and methods to estimate maximum-likelihood phylogenies: assessing the performance of PhyML 3.0. *Systematic Biology*, 59, 307–321.
- Guo, M., Bian, Y., Wang, J., Wang, G., Ma, X. & Xu, Z. (2017) Biological and molecular characteristics of a novel partitivirus infecting the edible fungus *Lentinula edodes*. *Plant Disease*, 101, 726–733.
- Hantula, J., Mäkelä, S., Xu, P., Brusila, V., Nuorteva, H., Kashif, M. et al. (2020) Multiple virus infections on *Heterobasidion* sp. *Fungal Biology*, 124, 102–109.
- Heinzelmann, R., Dutech, C., Tsykun, T., Labbé, F., Soularue, J.-P. & Prospero, S. (2019) Latest advances and future perspectives in *Armillaria* research. *Canadian Journal of Plant Pathology*, 41, 1–23.
- Heinzelmann, R., Prospero, S. & Rigling, D. (2017) Virulence and stump colonization ability of *Armillaria borealis* on Norway spruce seedlings in comparison to sympatric *Armillaria* species. *Plant Disease*, 101, 470–479.
- Hollings, M. & Stone, O.M. (1971) Viruses that infect fungi. *Annual Review of Phytopathology*, 9, 93–118.
- Ihrmark, K., Johannesson, H., Stenström, E. & Stenlid, J. (2002) Transmission of double-stranded RNA in *Heterobasidion annosum*. *Fungal Genetics and Biology*, 36, 147–154.
- Jamal, A., Sato, Y., Shahi, S., Shamsi, W., Kondo, H. & Suzuki, N. (2019) Novel victorivirus from a Pakistani isolate of *Alternaria alternata* lacking a typical translational stop/restart sequence signature. *Viruses*, 11(6), 577.
- Jiāng, D., Ayllón, M. A., Marzano, S. L., Kondō, H., Turina, M., & ICTV Report Consortium (2022). ICTV virus taxonomy profile: Mymonaviridae 2022. *The Journal of general virology*, 103(11), <https://doi.org/10.1099/jgv.0.001787>.
- Kashif, M., Hyder, R., de Vega Perez, D., Hantula, J. & Vainio, E.J. (2015) Heterobasidion wood decay fungi host diverse and globally distributed viruses related to *Helicobasidium mompa* partitivirus V70. *Virus Research*, 195, 119–123.
- Katoh, K. & Toh, H. (2008) Recent developments in the MAFFT multiple sequence alignment program. *Briefings in Bioinformatics*, 9, 286–298.
- Kedves, O., Shahab, D., Champramary, S., Chen, L., Indic, B., Bóka, B. et al. (2021) Epidemiology, biotic interactions and biological control of Armillarioids in the northern hemisphere. *Pathogens*, 10, 76.
- Kile, G.A., McDonald, G.I. & Byler, J.W. (1991) Ecology and disease in natural forests. In: Shaw, C.G. & Kile, G.A. (Eds.) *Armillaria root disease. Agricultural handbook no. 691*. Washington D.C.: USDA Forest Service.
- Kim, M.-S., Heinzelmann, R., Labbé, F., Ota, Y., Elías-Román, R.D., Pildain, M.B. et al. (2022) Chapter 20 – *Armillaria* root diseases of diverse trees in wide-spread global regions. In: Asiegbu, F.O. & Kovalchuk, A. (Eds.) *Forest microbiology*. London/Oxford/Cambridge MA/San Diego: Academic Press.
- Koch, R.A., Wilson, A.W., Séné, O., Henkel, T.W. & Aime, M.C. (2017) Resolved phylogeny and biogeography of the root pathogen *Armillaria* and its gasteroid relative, *Guyanagaster*. *BMC Ecology and Evolution*, 17, 33.
- Kondo, H., Botella, L. & Suzuki, N. (2022) Mycovirus diversity and evolution revealed/inferred from recent studies. *Annual Review of Phytopathology*, 60, 307–336.
- Kondo, H., Hisano, S., Chiba, S., Maruyama, K., Andika, I.B., Toyoda, K. et al. (2016) Sequence and phylogenetic analyses of novel totivirus-like double-stranded RNAs from field-collected powdery mildew fungi. *Virus Research*, 213, 353–364.
- Kondo, H., Kanematsu, S. & Suzuki, N. (2013) Chapter 7 – Viruses of the white root rot fungus, *Rosellinia necatrix*. In: Ghabrial, S.A. (Ed.) *Advance in virus research*, Vol. 86. New York, NY: Academic Press, pp. 177–214.
- Koonin, E.V., Krupovic, M. & Dolja, V.V. (2023) The global virome: how much diversity and how many independent origins? *Environmental Microbiology*, 25, 40–44.
- Kuhn, J.H., Adkins, S., Agwanda, B.R., Al Kubrusli, R., Alkhovsky, S.V., Amarasinghe, G.K. et al. (2021) Taxonomic update of phylum *Negamaviricota* (*Riboviria*: *Orthomavirae*), including the large orders *Bunyavirales* and *Mononegavirales*. *Archives of Virology*, 166, 3513–3566.
- Legrand, P., Ghahari, S. & Guillaumin, J.J. (1996) Occurrence of genets of *Armillaria* spp. in four mountain forests in Central France: the colonization strategy of *Armillaria ostoyae*. *The New Phytologist*, 133, 321–332.
- Linnakoski, R., Sutela, S., Coetzee, M.P.A., Duong, T.A., Pavlov, I.N., Litovka, Y.A. et al. (2021) *Armillaria* root rot fungi host single-stranded RNA viruses. *Scientific Reports*, 11, 7336.
- Madsen, C.L., Kosawang, C., Thomsen, I.M., Hansen, L.N., Nielsen, L.R. & Kjær, E.D. (2021) Combined progress in symptoms caused by *Hymenoscyphus fraxineus* and *Armillaria* species, and corresponding mortality in young and old ash trees. *Forest Ecology and Management*, 491, 119177.
- Marçais, B., Husson, C., Godart, L. & Caël, O. (2016) Influence of site and stand factors on *Hymenoscyphus fraxineus*-induced basal lesions. *Plant Pathology*, 65, 1452–1461.
- Marchler-Bauer, A., Bo, Y., Han, L., He, J., Lanczycki, C.J., Lu, S. et al. (2016) CDD/SPARCLE: functional classification of proteins via subfamily domain architectures. *Nucleic Acids Research*, 45, D200–D203.
- Marxmüller, H. & Guillaumin, J.J. (2005) Description et distribution des armillaires européennes. In: Guillaumin, J.J., Legrand, P., Lung-Escarmant, B. & Botton, B. (Eds.) *L'armillaire et le pourri-dié-agaric des végétaux ligneux*. Paris: INRA.
- Mathews, D.H., Disney, M.D., Childs, J.L., Schroeder, S.J., Zuker, M. & Turner, D.H. (2004) Incorporating chemical modification constraints into a dynamic programming algorithm for prediction of RNA secondary structure. *Proceedings of the National Academy of Sciences of the United States of America*, 101, 7287–7292.
- Osaki, H., Sasaki, A., Nomiya, K. & Tomioka, K. (2016) Multiple virus infection in a single strain of *Fusarium poae* shown by deep sequencing. *Virus Genes*, 52, 835–847.
- Petrzik, K., Sarkisova, T., Starý, J., Koloniuk, I., Hrabáková, L. & Kubešová, O. (2016) Molecular characterization of a new monopartite dsRNA mycovirus from mycorrhizal *Thelephora terrestris* (Ehrh.) and its detection in soil oribatid mites (Acari: Oribatida). *Virology*, 489, 12–19.
- Prospero, S., Botella, L., Santini, A. & Robin, C. (2021) Biological control of emerging forest diseases: how can we move from dreams to reality? *Forest Ecology and Management*, 496, 119377.
- Prospero, S., Holdenrieder, O. & Rigling, D. (2003) Primary resource capture in two sympatric *Armillaria* species in managed Norway spruce forests. *Mycological Research*, 107, 329–338.
- Prospero, S., Holdenrieder, O. & Rigling, D. (2004) Comparison of the virulence of *Armillaria cepistipes* and *Armillaria ostoyae* on four Norway spruce provenances. *Forest Pathology*, 34, 1–14.
- Prospero, S., Rigling, D. & Holdenrieder, O. (2003) Population structure of *armillaria* species in managed Norway spruce stands in the Alps. *New Phytologist*, 158, 365–373.

- Redfern, D.B. & Filip, G.M. (1991) Inoculum and infection. In: Shaw, C.G. & Kile, G.A. (Eds.) *Armillaria root disease. Agricultural handbook No. 691*. Washington D.C: USDA Forest Service.
- Romaine, C.P. & Schlagnhauser, B. (1995) PCR analysis of the viral complex associated with La France disease of *Agaricus bisporus*. *Applied and Environmental Microbiology*, 61, 2322–2325.
- Sahu, N., Indic, B., Wong-Bajracharya, J., Merényi, Z., Ke, H.-M., Ahrendt, S. et al. (2023) Vertical and horizontal gene transfer shaped plant colonization and biomass degradation in the fungal genus *Armillaria*. *Nature Microbiology*, 8, 1668–1681.
- Sasaki, A., Nakamura, H., Suzuki, N. & Kanematsu, S. (2016) Characterization of a new megabirnavirus that confers hypovirulence with the aid of a co-infecting partitivirus to the host fungus, *Rosellinia necatrix*. *Virus Research*, 219, 73–82.
- Sato, Y., Caston, J.R., Hillman, B.I., Kim, D.-H., Kondo, H., Nibert, M. et al. (2023) Reorganize the order *Ghabrivirales* to create three new suborders, 15 new families, 12 new genera, and 176 new species. ICTV pending proposal. <https://ictv.global/files/proposals/pending?fid=11741#block-teampus-page-title>
- Sato, Y., Shamsi, W., Jamal, A., Bhatti, M.F., Kondo, H., Suzuki, N. et al. (2020) Hadaka virus 1: a Capsidless eleven-segmented positive-sense single-stranded RNA virus from a phytopathogenic fungus, *Fusarium oxysporum*. *mBio*, 11, e00450-20.
- Smith, M.L., Bruhn, J.N. & Anderson, J.B. (1992) The fungus *Armillaria bulbosa* is among the largest and oldest living organisms. *Nature*, 356, 428–431.
- Sun, L., Nuss, D.L. & Suzuki, N. (2006) Synergism between a mycoreovirus and a hypovirus mediated by the papain-like protease p29 of the prototypic hypovirus CHV1-EP713. *The Journal of General Virology*, 87, 3703–3714.
- Sun, L. & Suzuki, N. (2008) Intragenic rearrangements of a mycoreovirus induced by the multifunctional protein p29 encoded by the prototypic hypovirus CHV1-EP713. *RNA*, 14, 2557–2571.
- Sutela, S., Poimala, A. & Vainio, E.J. (2019) Viruses of fungi and oomycetes in the soil environment. *FEMS Microbiology Ecology*, 95(9), f1119. <https://doi.org/10.1093/femsec/f1119>
- Telengech, P., Hisano, S., Mugambi, C., Hyodo, K., Arjona-López, J.M., López-Herrera, C.J. et al. (2020) Diverse partitiviruses from the phytopathogenic fungus, *Rosellinia necatrix*. *Frontiers in Microbiology*, 11, 1064.
- Thapa, V., Turner, G.G., Hafenstein, S., Overton, B.E., Vanderwolf, K.J. & Roossinck, M.J. (2016) Using a novel Partitivirus in *Pseudogymnoascus destructans* to understand the epidemiology of white-nose syndrome. *PLoS Pathogens*, 12, e1006076.
- Travadon, R., Smith, M.E., Fujiyoshi, P., Douhan, G.W., Rizzo, D.M. & Baumgartner, K. (2012) Inferring dispersal patterns of the generalist root fungus *Armillaria mellea*. *New Phytologist*, 193, 959–969.
- Tsykun, T., Rigling, D., Nikolaychuk, V. & Prospero, S. (2012) Diversity and ecology of *Armillaria* species in virgin forests in the Ukrainian Carpathians. *Mycological Progress*, 11, 403–414.
- Tsykun, T., Rigling, D. & Prospero, S. (2013) A new multilocus approach for a reliable DNA-based identification of *Armillaria* species. *Mycologia*, 105, 1059–1076.
- Turina, M., Lee, B., Sabanadzovic, S., Vainio, E.J., Navarro, B., Simmonds, P. et al. (2023) Create one new phylum, *Ambiviricota*, including one new class, one new order, four new families, four new genera, and 20 new species, in kingdom *Orthornavirae* (realm *Riboviria*). ICTV pending proposal. <https://ictv.global/files/proposals/pending?fid=11741#block-teampus-page-title>
- Urayama, S.-I., Katoh, Y., Fukuhara, T., Arie, T., Moriyama, H. & Teraoka, T. (2014) Rapid detection of *Magnaporthe oryzae* chrysovirus 1-A from fungal colonies on agar plates and lesions of rice blast. *Journal of General Plant Pathology*, 81, 97–102.
- Vainio, E.J. (2019) Mitoviruses in the conifer root rot pathogens *Heterobasidion annosum* and *H. parviporum*. *Virus Research*, 271, 197681.
- Vainio, E.J., Chiba, S., Ghabrial, S.A., Maiss, E., Roossinck, M., Sabanadzovic, S. et al. (2018) ICTV virus taxonomy profile: *Partitiviridae*. *The Journal of General Virology*, 99, 17–18.
- Vainio, E.J., Hakanpää, J., Dai, Y.C., Hansen, E., Korhonen, K. & Hantula, J. (2011) Species of *Heterobasidion* host a diverse pool of partitiviruses with global distribution and interspecies transmission. *Fungal Biology*, 115, 1234–1243.
- Vainio, E.J. & Hantula, J. (2016) Taxonomy, biogeography and importance of *Heterobasidion* viruses. *Virus Research*, 219, 2–10.
- Vainio, E.J., Müller, M.M., Korhonen, K., Piri, T. & Hantula, J. (2015) Viruses accumulate in aging infection centers of a fungal forest pathogen. *The ISME Journal*, 9, 497–507.
- Vainio, E.J., Pennanen, T., Rajala, T. & Hantula, J. (2017) Occurrence of similar mycoviruses in pathogenic, saprotrophic and mycorrhizal fungi inhabiting the same forest stand. *FEMS Microbiology Ecology*, 93(3), fix003. <https://doi.org/10.1093/femsec/fix003>
- Vainio, E.J. & Sutela, S. (2020) Mixed infection by a partitivirus and a negative-sense RNA virus related to myonnaviruses in the polypore fungus *Bondarzewia berkeleyi*. *Virus Research*, 286, 198079.
- Warwell, M.V., McDonald, G.I., Hanna, J.W., Kim, M.-S., Lalande, B.M., Stewart, J.E. et al. (2019) *Armillaria altimontana* is associated with healthy Western white pine (*Pinus monticola*): potential in situ biological control of the *Armillaria* root disease pathogen, *A. solidipes*. *Forests*, 10, 294.
- Wolf, Y.I., Kazlauskas, D., Iranzo, J., Lucia-Sanz, A., Kuhn, J.H., Krupovic, M. et al. (2018) Origins and evolution of the global RNA virome. *mBio*, 9(6), e02329-18.
- Xie, J. & Jiang, D. (2014) New insights into mycoviruses and exploration for the biological control of crop fungal diseases. *Annual Review of Phytopathology*, 52, 45–68.
- Yaegashi, H. & Kanematsu, S. (2016) Natural infection of the soil-borne fungus *Rosellinia necatrix* with novel mycoviruses under greenhouse conditions. *Virus Research*, 219, 83–91.
- Yang, S., Dai, R., Salaipeth, L., Huang, L., Liu, J., Andika, I.B. et al. (2021) Infection of two heterologous mycoviruses reduces the virulence of *Valsa mali*, a fungal agent of apple valsa canker disease. *Frontiers in Microbiology*, 12, 659210.

SUPPORTING INFORMATION

Additional supporting information can be found online in the Supporting Information section at the end of this article.

How to cite this article: Shamsi, W., Heinzelmann, R., Ulrich, S., Kondo, H. & Cornejo, C. (2024) Decoding the RNA virome of the tree parasite *Armillaria* provides new insights into the viral community of soil-borne fungi. *Environmental Microbiology*, 26(2), e16583. Available from: <https://doi.org/10.1111/1462-2920.16583>